UNIVERSITY OF OKLAHOMA

GRADUATE COLLEGE

EFFECT OF BIOMASS COMPOSITION ON HEMICELLULOSE, CELLULOSE, AND
LIGNIN DERIVED THERMAL PRODUCTS VIA TORREFACTION/PYROLYSIS

A THESIS

SUBMITTED TO THE GRADUATE FACULTY

in partial fulfillment of the requirements for the

Degree of

MASTER OF SCIENCE

By

REDWAN NAZIM
Norman, Oklahoma
2019

EFFECT OF BIOMASS COMPOSITION ON HEMICELLULOSE, CELLULOSE, AND
LIGNIN DERIVED THERMAL PRODUCTS VIA TORREFACTION/PYROLYSIS

A THESIS APPROVED FOR THE
SCHOOL OF CHEMICAL, BIOLOGICAL AND MATERIALS ENGINEERING

BY

Dr. Lance Lobban, Chair

Dr. Daniel Resasco

Dr. Steven Crossley

Dedication

This work is dedicated to:

Allah Subhanahu Wa Ta'ala ("The Most Glorified, The Most High")

who said

اقْرَأْ بِاسْمِ رَبِّكَ الَّذِي خَلَقَ

"Read! In the Name of your Lord, Who has created (all that exists)";

My MOTHER- whose love, support, and sacrifices can never be fully repaid, my father - whose encouragement and academic discipline are exemplary, and my brother – whose assistance and sheer belief in me are a gift beyond measure.

Thank you.

Acknowledgements

First and foremost, I am eternally grateful to *The One* above for gracing me with the opportunity to pursue my graduate studies at the only school I applied to, the University of Oklahoma, and blessing me with enough strength to navigate my way through the whole program.

I would like to place my sincerest and heart felt gratitude to my advisor, ***Dr. Lance L. Lobban***, for his continued guidance, support, and patience throughout my master's program, and especially for accepting me into such a program where I never thought I had the skill set nor the expertise required to be accepted. His willingness to offer a helping hand, in any way, shape, or form in both academic and non-academic related work is commendable. It has been an absolute honor and privilege to have had the opportunity to learn from such an admirable person.

I would also like to thank my committee members, ***Dr. Daniel Resasco*** and ***Dr. Steven Crossley***, for their contributions to my work. Over the years, they have helped me maneuver my way through this program and were always at hand to offer insightful suggestions and guidelines whenever asked.

It is crucial for me to express my gratitude to ***Rajiv Janupala***. Without his teachings, support, and patience, it would not have been possible for me to conduct this work. From showing me the nitty-gritty, and sometimes trivial, details of how to prepare samples to instructing me how to correctly operate the pyroprobe, his knowledge and wisdom were integral throughout the duration of my stay.

I must also thank ***Daniel Dixon*** – who worked with me when I first started out conducting research as an undergraduate student- for the numerous times he helped me troubleshoot the operating system, and Charles Crum for offering and sharing his thoughtful insights on my work while sharing the same office space.

Table of Contents

List of Tables

List of Figures

Abstract

Modern industrialization has resulted in an ever-increasing demand for petroleum-based fuel production and electricity generation. Exploitation of fossil fuel reserves have, however, raised grave environmental concerns due to rising carbon dioxide emissions in the atmosphere. While there is existing technology to generate electricity without having to combust coal or natural gas, there are severe engineering challenges at stake that hinder the production of a "carbon neutral" energy source capable of displacing petroleum-based fuels.

One option to counter act the engineering challenges to some extent is the thermochemical conversion of lignocellulosic biomass to produce biofuels. Due to its vast abundance in the Earth's surface, lignocellulosic biomass is a promising source of renewable energy source that is considered carbon neutral which can help dwindle the dependence on fossil fuels. Torrefaction/Pyrolysis of biomass is one thermochemical strategy with the ability to produce high yields of bio-oil; however, few unfavorable properties of bio-oils produced in such manner raise economic viability concerns due to the increasing costs associated with the upgrading/refining of the bio-oil and the resulting infrastructure required for such purification.

In this contribution, we consider the effects of heritable traits achieved on the thermochemical product streams of mutant and wild type (i.e. unmodified) switchgrass samples. This study incorporates genetic modification to understand and examine the broad thermal stability of lignin. It is hypothesized that mutant switchgrass samples exhibiting low *S/G* ratio will result in lower phenolic yields at low temperature thermal treatments without altering the total lignin content present within the biomass. By changing various process conditions (temperature and time) and calculating the cumulative yield of phenolic products per milligram of the raw biomass upon torrefaction and pyrolysis, it was observed that the hypothesis held its

ground. This approach helped develop a more thorough comprehension of which compositional features of the biomass are responsible for resulting thermochemical product distribution; such understanding will, in turn, allow catalytic valorization techniques to be customized for each specific product stream, thus making the process more economically viable.

Chapter 1 : Literature Review

1.1 Introduction

Modern industrialization, in conjunction with the emergence of crude oil as a cheap energy source, have heavily exploited fossil fuel reserves to satisfy the needs of fuel production and electricity generation. However, with increasing demand for non-renewable hydrocarbons in various industries, the focus has been turned to develop a sustainable energy source to ensure eradication of the dependence on fossil fuels. This objective has grown in impetus when major environmental consequences and political concerns (i.e. global carbon footprint) are considered; the burning of fossil fuels leads to the emission of carbon dioxide- among other detrimental gases- which is primarily responsible for global warming (1).

Considering the global energy consumption and growing environmental concerns, a conversion from non-renewable energy banks to renewable energy sources seem like the only rational choice; solar, wind, biomass, tide, wave, and geothermal energy reserves, therefore, become an attractive prospect. Of the renewable energy sources highlighted, energy derived from biomass has a unique advantage over other sources: it is the only energy source which is a sustainable carbon carrier (2). The Earth's surface harbors abundant biomass which makes it a tantalizing potential energy reserve; in addition to that, lignocellulosic biomass is considered to be carbon neutral since all the carbon within biomass comes from carbon dioxide in the atmosphere (which happens to be gaseous emission resulting from the burning of fuels); this atmospheric carbon dioxide is a raw material for biomass growth through photosynthesis, hence the net amount of atmospheric CO_2 is neutralized as a result of the carbon cycle (3).

1.2 Structure and thermal stability of biomass

Cellulose, hemicellulose, and lignin constitute the major segments of biomass. Cellulose and hemicellulose contribute anywhere from 60-90% of the biomass, while the remaining portion is majorly taken up by lignin (4,5). In addition to these components, organic extractives, inorganic minerals (ash), and water are also minor constituents of biomass (3,5). Cellulose is a crystalline glucose polysaccharide consisting of D-glucopyranose monomers units; these units are bonded through β-1,4 glycosidic linkages, as shown in Figure 1.1 (c). Hemicellulose, unlike cellulose, is a polysaccharide consisting of five different sugars; the most abundant constituent is a xylose polymer called xylan bonded at the 1 and 4 positions. Lignin, on the other hand, is a different type of polymer whose production is commenced by enzyme driven free-radical polymerization of alcohol precursors. Numerous "hydroxy-" and "methoxy-" substituted phenylpropane units make up the highly branched polyphenolic substance within the lignin molecule. Most lignin has coniferyl (*G*), sinapyl (*S*), and p-coumaryl (*H*) alcohol as their monomer units (3,4,5).
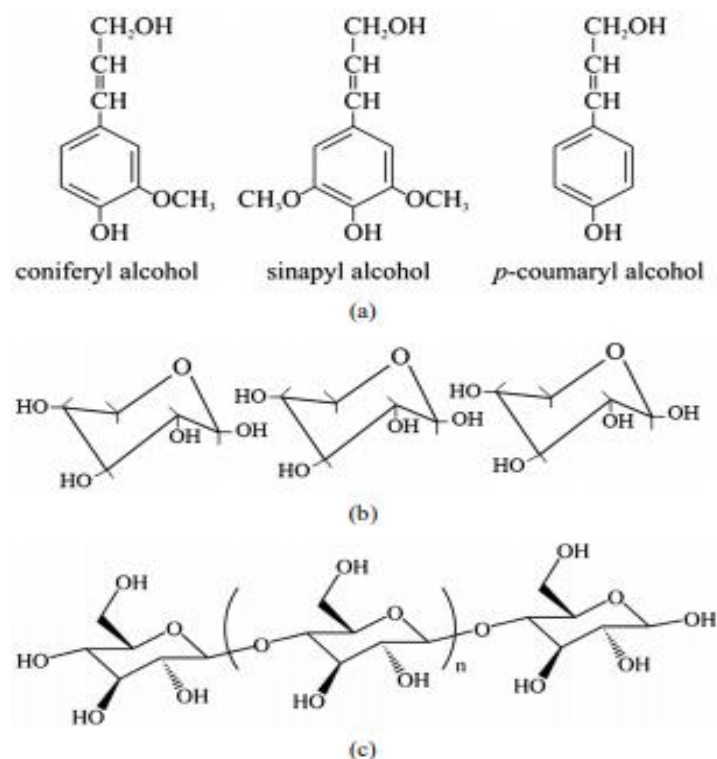
Figure 1.1: Structure of lignocellulosic biomass; (a) different monomer units comprising lignin; (b) xylose unit of hemicellulose; (c) cellulose (4)

Taking into consideration the different monomer units and their respective structures, each major constituent of biomass possesses different thermal decomposition features, which can be carefully exploited to extract valuable chemical compounds. Hemicellulose displays the lowest thermal decomposition temperature, and mainly degrades at temperatures ranging between 150 °C and 315 °C. Cellulose degrades between 315 °C and 400 °C, whereas lignin undergoes decomposition for temperatures ranging between 250 °C and 500 °C(3,6). The thermal decomposition ranges of each constituent of biomass is displayed in Figure 1.2.
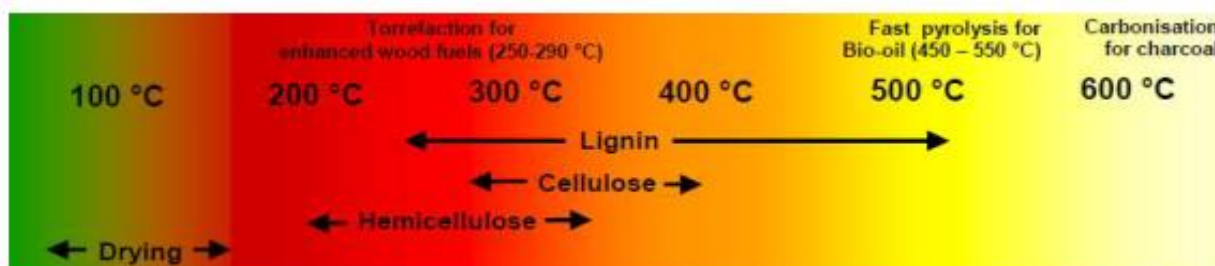
Figure 1.2: Thermal stability of the different constituents within lignocellulosic biomass (6)

1.3 Thermal conversion technologies

Thermochemical and biochemical conversion of biomass are two strategies that have been explored as viable options to displace petroleum-based fuels with the industrial production of liquid fuels. Thermochemical conversion involves the degradation of biomass in the absence of oxygen, and its subsequent condensation of organic products to manufacture bio-oil (which can then be refined and upgraded through various methods to produce liquid fuels similar in characteristics to diesel or gasoline). Biochemical conversion, on the other hand, entails the influence of enzymes to convert biomass contents into sugars followed by the usage of microbes to produce ethanol or other fuel molecules. Considering the two processes, thermochemical conversion has the potential ability to make use of all carbon-containing biomass components which would allow already existing industrial infrastructure to be utilized in the production for biomass derived fuels (7).

However, bio-oil derived from lignocellulosic biomass has high oxygen content, low energy density and low calorific value (relative to fossil fuels), and high moisture content. Biomass's hydrophilic and hygroscopic nature adds an additional layer of difficulty when it comes to biomass storage; moreover, comminuting the biomass into small, evenly sized particles is a difficult process which increases the cost of production (3,6). As a result, deploying biomass resources as chemical feedstocks faces adversities and the challenge is to determine a technology

4

which can be economically sustained (i.e. decreasing processing and upgrading costs, and improving fuel production while maintaining high carbon yield) for biomass conversion into fuels (and hence can compete with existing fossil fuel technologies).

Thermochemical conversion of lignocellulosic biomass has been touted as a possible strategy to manufacture biofuels (3,8). The two most heavily researched thermal degradation treatment processes are pyrolysis and torrefaction. Pyrolysis is the thermal decomposition of organic substances in the absence of oxidizing agents, while torrefaction is termed as a milder form of pyrolysis (i.e. carried out at lower temperatures). Depending on the type of product desired, the thermal treatment can be carried out at different temperatures for varying amounts of time (as depicted in the Figure 1.3) (8).

At pyrolysis temperatures, the majority of solid biomass is rapidly converted to liquid biofuels (up to 75%); the remaining portion of the biomass is converted to non-condensable gases such as CO, CO_2, and H_2, and solid carbonaceous char. The immediate vapor products upon thermal degradation are carried away from the reactor with the help of a carrier gas to ensure minimal secondary reactions taking place, which could be catalyzed by particles within the leftover char (6,8). A lower temperature thermal degradation – otherwise known as torrefaction – associates the thermal degradation of biomass at a reactor temperature of approximately 290 °C (with a residence time ranging from a couple of minutes to even hours). The overwhelming result of torrefaction (which removes water, carbon dioxide, and light oxygenates) is a solid product (up to 77%) that has a higher energy density and lower moisture retaining capability than the original

biomass sent into the reactor (8). During this process, the partial de-volatilization of the biomass reduces its weight and decreases the O/C ratio of the biomass.

Mode	Conditions	Liquid	Solid	Gas
Fast	Reactor temperature 500°C, very high heating rates > 1000°C/sec, short hot vapour residence ~1 s	75%	12% char	13%
Intermediate	Reactor temperature 400-500°C, heating rate range 1 – 1000°C/sec, hot vapour residence ~10-30 s	50%	25% char	25%
Slow – Torrefaction	Reactor temperature ~290°C, heating rate up to 1°C/sec, solids residence time ~30 min	0-5%	77% solid	23%
Slow – Carbonisation	Reactor temperature 400-500°C, heating rate up to 1°C/sec, long solid residence hrs – days	30%	33% char	35%

Figure 1.3: Different thermal degradation conditions and their respective overall product distribution (8)

1.4 Features of Bio-oil

The bio-oil produced through thermal degradation has high carbon content and can be utilized for heat and power generation, or the torrefied biomass can be used as chemical feedstock (i.e. improved biomass) for further pyrolysis (6,8). However, there are some drawbacks to the bio-oil which hinders its usage as a transportation fuel. Firstly, these bio-oils have high oxygen content which makes them highly reactive; the carboxylic groups can interact readily to form esters and oligomers – these lead to increased processing costs during storage, and such reactions increase the molecular weight and viscosity of the oil which ultimately results in phase separation. In addition to this, bio-oils have high moisture and acid content, which result in low heating values and corrosion of industrial pipelines and vessels respectively (6). Due to such characteristics, bio-oils are immiscible with hydrocarbon fuels, hence its viable integration with existing refinery systems is not possible.

The above concerns can be addressed through catalytic conversion of bio-oils in refineries. Hydrotreating the bio-oil is a possible strategy to decrease the oxygen content; however, hydrotreating is associated with increased hydrogen input costs and decreased carbon efficiency. An alternative to hydrotreating is the use of zeolite catalysts for bio-oil upgrading. However, the carbon efficiency challenge is not necessarily resolved through this route due to the rapid deactivation of the catalyst as a result of coke formation (6). Therefore, it is critical to think of a bio-oil upgrading method which minimizes hydrogen consumption and maximizes carbon retention.

1.5 Staged Thermal Fractionation

One method which has been explored is the segregation of intermediate streams of thermal degradation products with enhanced purity compared to pyrolysis product streams through staged thermal fractionation. This process exploits the thermal stability of each main constituent of biomass and produces decomposition products at different temperatures; the disruption to the structures/properties of the different biopolymers present within the biomass at those temperatures is minimal. One example of a staged strategy is to deploy an initial low temperature thermal degradation step (stage 1) targeting hemicellulose decomposition, followed by an intermediate temperature degradation (stage 2) for cellulose decomposition, and finally a high temperature thermal treatment (stage 3) – mimicking fast pyrolysis conditions- to decompose the remaining lignin within the biomass (Figure 1.4). The logic behind such a move is the expected enhanced purity volatile products of each main biopolymer, which could then be subsequently subjected to catalytic treatments for economical upgrading process.
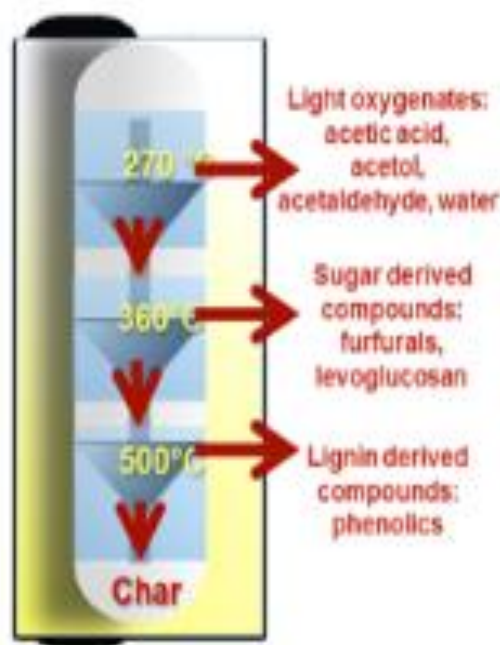
Figure 1.4: Staged thermal fractionation displaying respective volatile stream products (extracted from a manuscript in preparation)

Segregation of thermochemical degradation products of lignocellulosic biomass (specifically switchgrass for the purposes of this thesis) can be improved via process and feedstock compositional factors. This thesis, in particular, will focus on determining how alterations in starting biomass feedstock composition (specifically changes in the lignin biosynthesis pathway) influence decomposition products at low temperature thermal treatments. The purpose of this research is to study the effects of heritable traits (achieved via genetic modification) within switchgrass samples on low temperature thermal degradation products.

1.6 Motivation

A desirable separation to accomplish is the "clean" removal of hemicellulose via a low-temperature staged thermal fractionation treatment (stage 1). While previous studies have shown that such segregation can be achieved using temperature and time constraints (270 °C with a residence time of 20 minutes), cellulose-derived and lignin-derived volatiles were also present

(7). This stage 1 treatment could potentially be altered to minimize cellulose degradation through the exploitation of temperature and residence time parameters; however, TGA studies have indicated that it is impossible to suppress lignin decomposition at lower temperatures suited for hemicellulose degradation (7,9). One option to minimize lignin-derived thermal products at low-temperature treatment is to utilize a biomass feedstock with a low-lignin content. Such a move would, however, decrease the total lignin-derived phenolics from the overall thermal treatment procedure. Instead, genetic modification might alter the thermal stability of lignin to minimize its degradation at lower temperatures (without reducing the total amount of lignin in the starting biomass feedstock. In this research, the differences in the compositional product streams upon various thermal treatments of raw (i.e. unmodified) and genetically modified switchgrass will be studied. The study hypothesizes that genetically modified switchgrass will exhibit lower phenolic yields due to suppression of lignin decomposition at low temperature thermal treatments.

Chapter 2 : Experimental methods and Analytical techniques

2.1 Sample preparation

For the thermal degradation experiments (i.e. torrefaction and/or pyrolysis), biomass samples were prepared by loading a certain amount of the biomass (ranging between 0.50 mg and 2.20 mg) into a fire polished quartz tube *(CDS Analytical, Oxford PA, Part No. 10A1-3015)*. The quartz tube used in the experiments were open ended on both sides; hence, a filler rod *(CDS Analytical, Oxford PA, Part No. 10A1-3016S)* is inserted within the quartz tube to seal the bottom end. To further consolidate the placement of the biomass, and to prevent any loss of the biomass through the sides and bottom of the quartz tube, a small amount of quartz wool *(CDS Analytical, Oxford PA, Part No. 0100-9014)* is placed on top of the filler rod where the biomass sample rests. Biomass sample is sucked into the tube using vacuum. The figure below illustrates a typical biomass sample tube (7). The quartz tubes are weighed before and after the loading of biomass, and the difference between the weights is taken as the mass of biomass within the tube. The weighing measurements are done on a Mettler Toledo XS105 Dual Range balance (maximum weighing capacity of 120g with a linearity of ±0.2 mg).
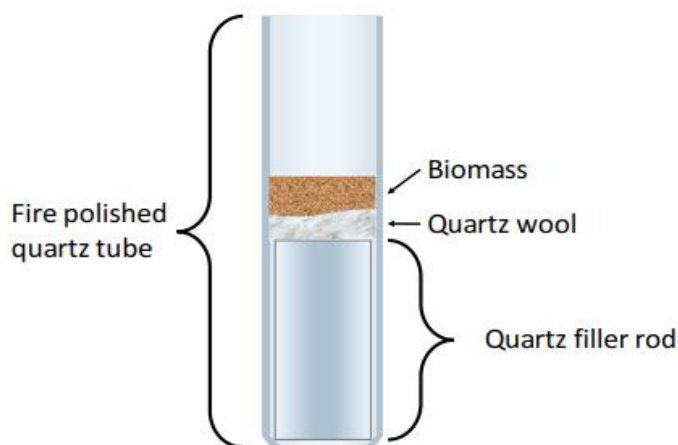
Figure 2.1: A typical sample tube for thermal degradation experiments (7)

2.2 Torrefaction/Pyrolysis apparatus

The thermal decomposition of biomass was carried out in a CDS Analytical Pyroprobe 5250T. The top portion of the pyrolysis autosampler contains a revolving carousel; the carousel incorporates multiple slits/holes where the biomass samples are loaded onto. The quartz tubes, which contain the biomass, are positioned vertically in the carousel. A collection tray is located beneath the torrefaction/pyrolysis system, and it collects tubes after they are "spent" in the pyrolysis chamber. Figure 2.2 shows a schematic diagram of the system.
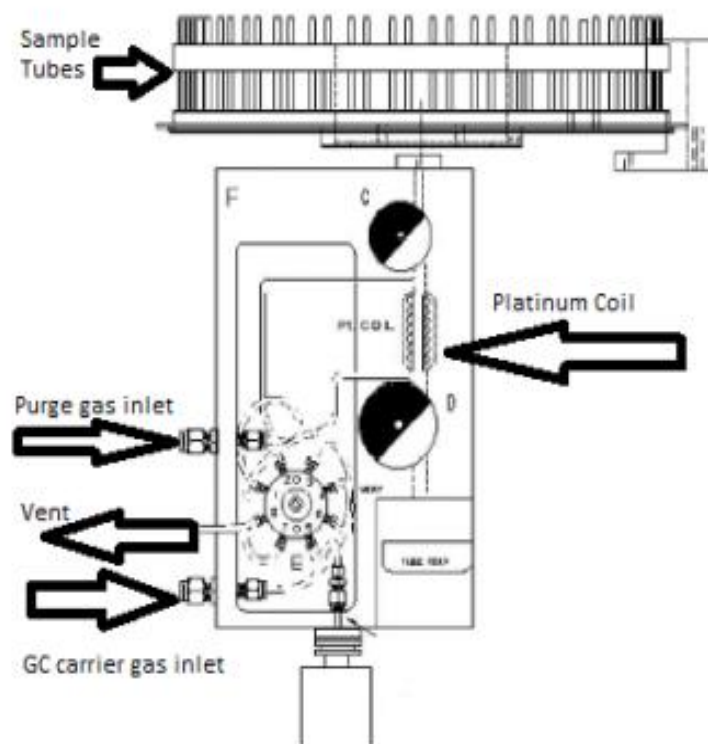
Figure 2.2: Schematic of 5250T pyroprobe system with autosampler

Once the "GC ready" signal is activated in the software, the autosampler carousel advances, and drops the sample tube on top of an inlet valve. This inlet valve rotates to allow the sample tube to further drop into the pyrolysis chamber – which rests on top of an outlet valve. Once the tube is within the chamber, the top valve closes, and the pyrolysis chamber is purged with helium gas for 20 seconds; this removes any air that might have been introduced into the chamber while samples were being dropped. This purge is subsequently followed by the heating of the pyrolysis chamber; platinum filament wires are wrapped around the surface of the glass pyrolysis chamber, and it is resistively heated to the configured set point of the instrument using a $1000℃/s$ temperature ramp. After the residence time of the biomass sample has elapsed, the platinum filament gets deactivated, and the outlet valve beneath the chamber opens to allow the sample quartz tube to drop into the collection tray. The picture below (Figure 2.3) depicts the pathway taken by the sample tube (which is otherwise obscured by a protective insulating cover) once it has been dropped from the autosampler carousel. For same samples which undergo various successive thermal treatments, the sample tube is left within the pyrolysis chamber after it undergoes first thermal treatment; once the gas chromatography program is completed (which takes approximately 100 minutes), the sequence of steps resumes from the purge step since no new tube has been dropped from the carousel. The tube is only dropped into the collection tray once all thermal treatments have been completed within the pyrolysis chamber. Once a tube is dropped into the collection tray, the chamber is cleaned via the reactivation of the platinum filament; the chamber is held at a temperature of 1200 ℃ for 20 seconds while a sweeping flow of helium gas is purged through the chamber at around 30 $\frac{ml}{minute}$.
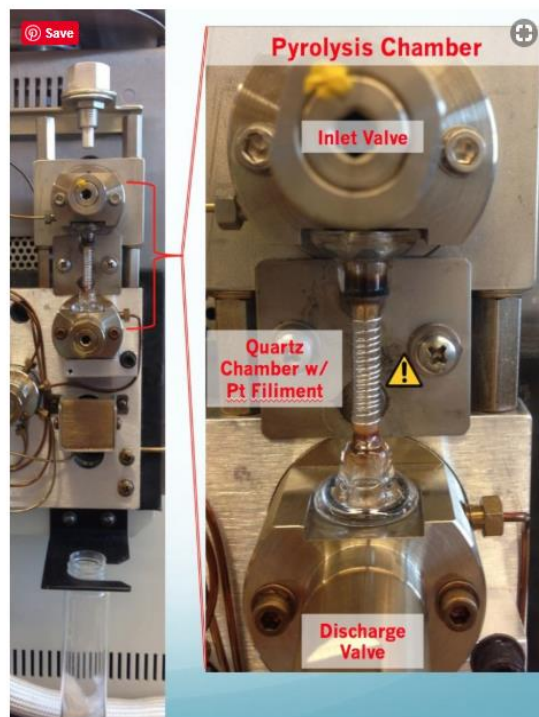
Figure 2.3: Pathway of a sample tube through the pyrolysis chamber

All thermal degradation experiments (i.e. torrefaction and pyrolysis steps) utilized helium as a carrier gas at one atmosphere. This flow is monitored and regulated by the gas chromatograph (GC) attached to the CDS Analytical 5250T pyroprobe system. For all experiments carried out, the total flow rate of helium through the system was maintained at $14\ \frac{ml}{minute}$. This flow rate was a direct result of the split ratio within the GC column being maintained at 10:1 for all thermal degradation experiments; it was determined that regulating the split ratio at this level ensured a sufficient amount of thermochemical products being detected by the GC.

A side view of the tubing within the pyroprobe valve oven (which is otherwise obscured by an insulating cover) shows the possible paths that evolved vapors of thermochemical products can take once the biomass has been torrefied or pyrolyzed (i.e. exits the pyrolysis chamber). Figure

2.4 displays the network of tubing within the valve oven – which is held at 350℃ during pyroprobe operation. Torrefaction/Pyrolysis vapors can directly be carried to the GC via a transfer line (depicted by the green arrow in Figure 2.5) or the evolved volatiles can first be trapped in the hydrocarbon trap (the hydrocarbon trap is the white box on the top left of the instrument as can be seen in Figure 2.4) – which is cooled with liquid nitrogen- before being transferred to the GC. For the purposes of this thesis, the trap option was never utilized.

Figure 2.4: Valve oven within the pyroprobe system
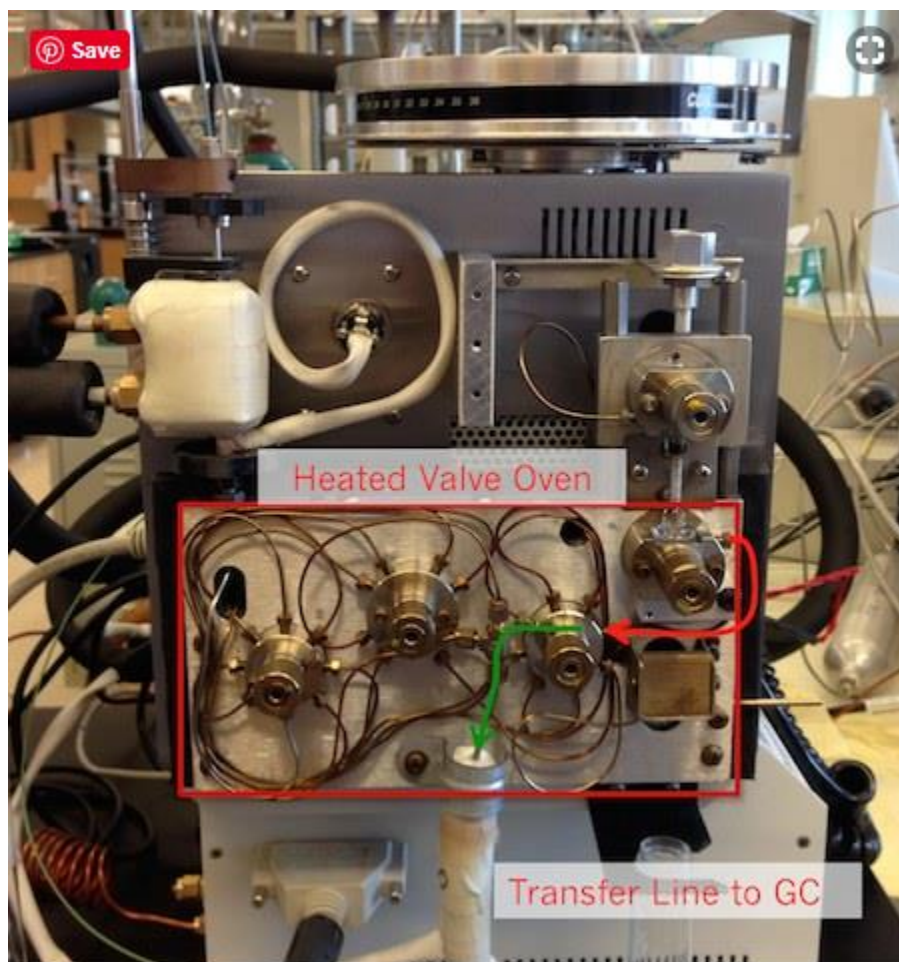
Figure 2.5: Pathway of evolved vapors going directly into the transfer line (green arrow) once they leave the pyrolysis chamber (red arrow)

2.3 Gas Chromatography

The thermochemical volatiles exiting the pyrolysis chamber travel to the GC column via a 1/16 inch Silco Steel transfer line; the temperature of the transfer line is maintained at 350 ℃, and it is connected to the injection port of a Shimadzu QP2010S + GC/MS-FID system *(Shimadzu Corporation, Kyoto, Japan)*. The GC/MS-FID system is equipped with a 60-meter semi-polar Restek *(Restek Corporation, U.S., Bellefonte, PA)* RTX-1701 column; the column's thickness and diameter are both 0.25 µm. The temperature at the injection port is maintained at 280℃. The temperature program in the column begins at 45℃ for 2 minutes. The temperature is then

increased at a rate of 3K per minute for approximately 78.33 minutes to a final temperature of 280℃. It is kept at this temperature for 20 minutes (the total program time comes out to be 100.33 minutes). The pressure at the injection port is set at 16.7 psi, while the column flow is strictly maintained at 1 $ml/minute$. The mass spectrometer starts scanning masses at 35.00 m/z and ends scanning masses at 250 m/z at 0.5 seconds per scan. The start time of the mass spectrometer is 4.58 minutes and end time is 94.33 minutes. The ion source temperature within the mass spectrometer is kept at 200℃, while the interface temperature is kept at 250℃. All the analysis presented in this thesis has utilized the same GC column temperature program, mass spectrometer settings, and FID settings. The resulting ion chromatograms from MS and FID are used to identify and quantify significant peaks within the respective chromatograms.

2.4 Compound identification

Two publications by Faix et al. (10,11) were used as primary sources for the identification of the chemical compounds upon thermal degradation of biomass. Faix et al. used a 15m DB-1701 column (the same type of column used in the data analysis for this thesis) to conduct his findings; consequently, the retention order of the torrefaction/pyrolysis products that was observed would be the same as in this study. It is important to note that the absolute time for the observed chemical compounds in Faix et al. study will not be the same as this study due to the variation in the length of the columns being used within the GC. Base peak (intensity 100%) of each identified chemical compound is provided in the publication; this is accompanied with intensities of nine other abundant masses to facilitate the compound identification process. When peaks were proving to be difficult to be identified using the two publications, the in-built NIST library search within the GC-MS software was utilized for compound identification; in some cases, peaks were assigned to compound lumps based on major ions or left unidentified when aforementioned resources were

already exhausted. Figure 2.6 illustrates the methodology behind compound identification (7). The identified peaks in the MS chromatogram were then matched through visual observation to their corresponding peaks in the FID chromatogram. The area of each peak within the FID chromatogram was determined through the integration tool in the Shimadzu GC Solutions software. The peak areas obtained from the FID chromatogram was divided by the total amount of biomass (i.e. mass) present within the sample tube, thereby normalizing each sample to the initial amount of sample fed into the pyroprobe system.
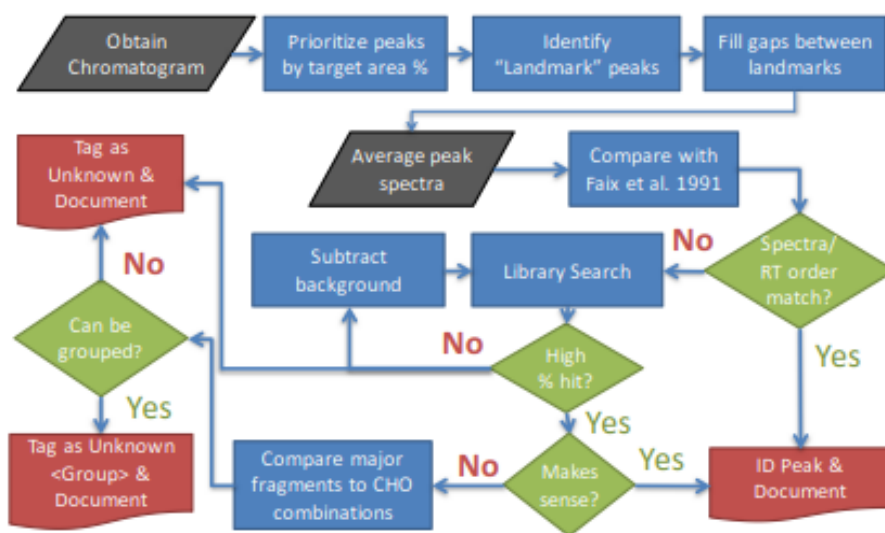
Figure 2.6: Methodology for compound identification being illustrated through a flowchart; landmark peaks include, but are not limited to, acetic acid, furfurals, levoglucosan (anhydrous sugars) (7)

2.5 Lumping approach

Based on characteristics (i.e. organic functionalities) of successfully identified compounds, they were further categorized into lumps of compound groups – in a similar fashion to what is described by Dauenhauer et al. (12). This type of classification made it simpler and easier to measure the carbon content present in each diverse compound group. The lump of compounds that were formed for this study are: light oxygenate, carbon dioxide, acetic acid,

furfurals, furans, alkyl benzenes, alkyl phenols, anhydrous sugars, and methoxy phenols. Light oxygenate refers to chemical compounds which contained at least one oxygen molecule within their structural framework (e.g. straight carbon chain molecule) but lacked the presence of an aromatic (i.e. ring-like) compound. Carbon dioxide and acetic acid (carboxylic acid containing an acetyl group and a hydroxyl group) were kept as separate entities as they represented major, dominant peaks (i.e. easily distinguishable through visual observation) in FID chromatograms when compared to other peaks representing chemical compounds classified within the other compound lumps. Four carbon atoms in the presence of a solitary oxygen atom engulfed in an aromatic ring constitutes a furan molecule; addition of an aldehyde group to this structure results in the formation of furfurals. Derivatives of benzene in which one or more hydrogen atoms are replaced by alkyl groups are classified as alkyl benzenes; they are a subset of aromatic hydrocarbons (e.g. toluene). Similarly, alkylation of phenols constitutes the family of organic compounds known an alkyl phenols. Often a major product of biomass thermal degradation is levoglucosan – a bridged polyhydroxy heterocyclic compound and a member of the anhydrous sugars- which is a six-carbon ring compound with three alcohol functional groups. Phenol molecules with a methoxy functional group attached to it (i.e. methyl group bound to oxygen) makes up methoxy phenols. From here onwards, product yields of torrefaction/pyrolysis experiments will be reported in terms of the lump of compound groups. Table 1 in the appendix list all the compounds, and the subsequent family groups they were categorized in, that were identified throughout the course of this study. The total mass (per mg of raw biomass) or carbon content – depending on what is reported- was summed for each of the compounds within the lump. The mean values of these compound lumps across the technical replicate experiments performed for this study are reported throughout this thesis as "yield".

2.6 FID Quantification

To perform FID calibration, varying concentrations of phenol were dissolved in methanol at known quantities to develop a response curve. Relative response factors – that were obtained from literature (when available)- in conjunction with the response curve developed, was utilized to determine the carbon content of each identified thermochemical product in the MS/FID chromatograms.

The quantification of bio-oil, in terms of thermochemical products, is performed through the Flame ionization detector (FID). Response factors (RF) are required to measure the amount of different chemicals present within the bio-oil. Response factors are defined as the following:

$$RF = \frac{area\ of\ sample}{mass\ of\ sample}\ (Equation\ 1)$$

Response factor values are dependent on the molecular structure of the chemical compound, and they vary for different compounds. Relative response factors (RRF), is simply the ratio of the response of two different chemical compounds (one of them being an internal standard compound). In literature, n-heptane is usually utilized as the internal standard (14,15). It is defined as the following:

$$RRF = \frac{RF_{sample}}{RF_{internal\ standard}}\ (Equation\ 2)$$

The Relative Response Factor is dependent on the structural moiety of the chemical compound and the internal standard being used; operating conditions have no influence on RRF. As a result, reported RRF values in the literature would be similar to the compounds being identified in this study – any differences would be attributed to experimental errors, impurity of compounds being used, and/or possible decomposition on injection or adsorption by the GC column (16). Response factors are deemed to be constant for such quantification since FID's

response for organic compounds is linear with concentration over a substantial range (17). Additionally, FID's response is stable and is unhindered by changes in the flow rates of carrier gas (18).

Due to the unavailability of RF values of each single component identified in MS/FID chromatograms, a model correlating the chemical structure with the RF values was developed at the University of Oklahoma (13). This model is based on the concept of Effective Carbon Number (ECN) – which was first introduced by Sternberg et al. and is defined as the following:

$$ECN = 7 * \frac{\dfrac{area\ sample}{area\ n - heptane}}{\dfrac{mole\ sample}{mole\ n - heptane}} = 7 * \frac{RF_{sample} * MW_{sample}}{RF_{n-heptane} * 100}\ (Equation\ 3)$$

In the above equation, "MW_{sample}" refers to the molecular weight of the sample compound; the numerical value 7 is n-heptane's ECN value (19).

When developing the OU ECN model, literature was exhaustively considered to find FID response factors for different chemical families. Katrizky et al. conducted a QSPR (quantitative structure-property relationship) study which correlated the chemical structure of a compound with the response factor of approximately 150 compounds in a wide range of chemical families. These RF values were fit to 6 best descriptors – prominent among which are the number of carbons connected to C or H only, and the total molecular one-center one-electron repulsion energy. This study is described in (15). In brief, response factors for numerous organic chemical compounds were collected from various literature sources; each chemical compound was classified into a specific type depending on the position of each carbon atom within the molecule (i.e. aliphatic, carbonyl, ether, primary/secondary/tertiary alcohol, ester, etc.), and a linear model was developed as a fit to predict the ECN from the number of each type of carbon atom.

While Sternberg (19) estimated the RF values, and subsequent ECN contributions, for different types of functionalities, that study did not incorporate all types of functionalities that need to be accounted for when biomass is thermally degraded to produce bio-oil. Functionalities such as furanics and phenolics – which are present in substantial amount when torrefaction/pyrolysis experiments are carried out- were not present within that study. As a result, a model needed to be developed that included the different functionalities this thesis would encompass. While the model to predict the ECN contributions for different types of functionalities was being developed at OU, it was found that Relative Response Factor (RRF) values were widely available for a vast array of different chemical compounds in literature. Those RRF were used in tandem with the experimental data obtained at OU to fully develop an ECN model encompassing all interested chemical compounds and functionalities. Three different sources – Katrizky et al. (15), Dietz et al. (14), and Meier et al. (20) – were utilized to estimate RF values – which is directly proportional to RRF. By minimizing the sum of the squared differences between reported values and predicted values, the OU ECN contributions (i.e. measured values) were found to be in good agreement with the predicted values. Details into the thought process and reasonings behind different sources for the OU model (including parity plots to show the effectiveness of the developed model) is explained in detail in (13). Figure 2.7 lists the ECN contribution of different functionalities from the OU developed model (13). Table 2 in the Appendix lists all individual compounds identified in FID chromatograms with their respective ECN contribution and Response Factor (RF).

Aliphatic C	0.98
Aromatic C	0.94
C attached to arometic ring	0.84
Acid C	-0.30
Carbonyl C	-0.07
C_OH primary alcohol	0.48
C_OH secondary alcohol	0.40
C_OH tertiary alcohol	0.88
C_OH phenolic	0.12
Ether C	0.28
Ether C ring (furans, pyrans…)	-0.52
Ester	-0.46
Ether attached to aromatic ring	-0.02

Figure 2.7: ECN contributions of different functionalities from OU developed model

Chapter 3 : Relationships between biomass composition and their respective thermal degradation products

3.1 Biomass Composition

To comprehend the broad association between biomass composition and resulting bio-oil composition, it is important to acknowledge the role played by the chemical structure of the biomass and the many interactions within the major cell wall components making up the biomass. The structure of a plant (i.e. leaves and stem) is primarily determined by the cell walls, and they are mainly composed of cellulose, hemicellulose, and lignin (structural proteins and minerals are also present to a lesser extent) (7, 21-23). For instance, dry switchgrass – the bioenergy crop under consideration for this thesis – comprises approximately 70% cell walls, 9% intrinsic water, 8% minerals, 6% proteins, and 5% nonstructural sugars (23). The discussion forward will mainly focus on the components of secondary cell walls since they constitute the majority of plant biomass (24). Figure 3.1 provides the list of individual components with their weighted percentages that make up plant biomass for bio-oil conversion. The subsequent figure displays the chemical structures (with the carbon atoms being numbered) of the most abundant individual components of biomass.

Biomass Component	Dry Wt (%)[a]
Cellulose	15-49 [b]
Hemicellulose:	12-50 [b, c, d]
Xylan	5-50 [c]
Mixed Linkage Glucan	0-5 [c, e]
Xyloglucan	Minor [c]
Mannan (and galactoglucomannan)	0-30 [c, f]
Soluble (Mainly sucrose)	9-67 [b, g]
Pectin	< 0.1 [h]
Lignin	6-28 [b]
Ferulic acid and *p*-coumaric acid	< 1.5 [h]
Protein	4-5 [b]
Ash (Mainly silicate)	0.4-14.4 [b]
Intrinsic moisture	11-34 [i]

[a]Percent mass composition of secondary cell walls. [b](40) [c](41) [d]As the highest percentage of xylan in (41) is higher than the highest percentage of hemicellulose in (40), the highest percentage of hemicellulose is set to the highest percentage of xylan. [e]MLG is only abundant in grasses, The maximum percentage of MLG we are aware of is that of the mature rice stem after flowering. (42) [f]Galactoglucomannan is only abundant in gymnosperm woods. Dicots and grasses possess <8% of mannan and galactoglucomannan. (41) [g]The high solubles abundance is only for sorghum biomass. Other plants usually have less than 15% soluble content. (40) [h](43) i (44)

Figure 3.1: Distribution of individual biomass components within vascular plants (7)
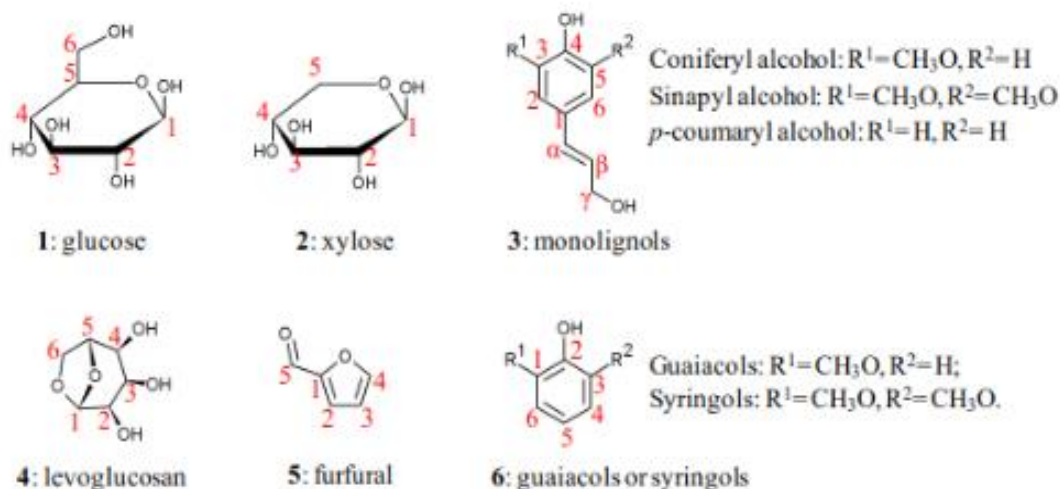
Figure 3.2: Chemical structures highlighting the carbon atoms of major basic units present within biomass polymers and related thermal degradation products (7)

As Figure 3.1 depicts, cellulose constitutes anywhere between 15 – 49% of biomass by dry weight. In plant cell walls, cellulose is primarily present in the form of insoluble microfibrils which typically comprise approximately 36 hydrogen-bonded chains; these chains contain β-

(1,4)-linked glucose units (unbranched polymer ranging anywhere between 500 and 14,000 molecules) (7,25).

Hemicellulose is the second most abundant species present within cell walls (ranging between 12-50% of biomass by dry weight), according to Figure 3.2. Hemicelluloses are heterogeneous branched polysaccharides containing numerous monomeric units of various sugars and acyl groups (7,26). Taxonomic divisions (e.g. grasses, dicots, softwoods) within the plant species influence the monomeric units available in the hemi cellulosic polysaccharides. Switchgrass – the primary biomass subject for this thesis- is categorized under grasses hemicellulose division, within which the most abundant component is mixed-linkage glucan (MLG) and glucuronoarabinoxylan (GAX) (7,27). MLG is an unbranched glucose polymer comprising both β-(1,3)- and β-(1,4)- linkages (27), and is almost exclusively found in grasses (7). Xylans, on the other hand, comprise β-(1,4)- linked xylose backbone with different substitutions (e.g. glucuronic acid, 4-O-methyl glucuronic acid) via α-(1-2)- linkages. GAX, for instance, in addition to being substituted by glucuronic acid, are substituted by arabinofuranoses at the O-3; these can be further substituted by phenylpropanoid acids to make feruloyl- and p-coumaryl esters bonded at the O-5 (26). Xylans are primarily composed of pentoses while mannans consist of hexoses like mannose, glucose, and galactose. Although not abundantly present in secondary walls, xyloglucan and pectins are two other minor polysaccharides available within cell walls; xyloglucan consists of β-(1-4)- linked glucose residues while pectin is a polymer (branched or unbranched) rich in several monosaccharide residues (7, 26).

Lignin makes up the third most abundant component of biomass. Lignin is a crosslinked polymer which is primarily composed of three monolignol monomers: *p*-coumaryl alcohol, coniferyl alcohol, and sinapyl alcohol (28). These lignols are incorporated within the lignin

biosynthesis network in the form of phenylpropanoids p-hydroxyphenyl (***H***), guaiacyl (***G***), and syringyl (***S***), respectively (29). These various types of incorporated groups within the lignin biosynthesis network, along with its structural heterogeneity, give rise to different depolymerization reactions during thermal degradation treatments (7). The three major lignin monomer units are "methoxylated" to different degrees in their carbon ring. ***H*-**monomer units lack ring methoxy groups; ***G*-**monomer units contain one methoxy group at the O-3 position while ***S*-**monomer units are methoxylated at both O-3 and O-5 ring positions (29), as displayed in Figure 3.2. These monomer units tend to undergo oxidative coupling reactions within the cell wall to create different types of dimers; these dimers include, but are not necessarily limited to, β-O-4, β-5, β-β, 5-5, 5-O-4, and β-1. The oxidative coupling reactions allow other atoms within the network to further polymerize themselves, thereby increasing the structural heterogeneity of lignin. It is worth noting that lignin units have the capability to be esterified with p-coumaryl, p-hydroxybenzoyl, and acetyl groups – primarily at the γ position of terminal monomer units (30,31). The acylation degrees and overall lignin composition within the biomass vary among plant clades (7). For instance, grass lignin – which is the primary focus of this thesis- contains high levels of p-coumarate esters (32), and possesses the ability to be etherified by tricin and ferulic acid (33, 34).

Inorganic minerals such as Ca, K, Si, Mg, Al, S, Fe, P, Cl, Na, and some trace amounts of Mn and Ti are also present in biomass; these inorganic elements are formed through the oxidation of biomass at 575 ℃ (35,36). The abundance of the mineral elements is dependent upon the species of biomass (i.e. taxonomic divisions); for instance, grass biomass (e.g. switchgrass) generally contains more Cl, K, S, and Si compared with woody biomass – which incorporates more Ca (36).

Although individual biomass components are sometimes devoid of physical interaction, covalent and non-covalent interactions allow individual constituents to correlate; correlation is also possible due to the components being present within the same plant organ or by virtue of being in the same developmental stage of the plant. The thermal degradation products from one biomass constituent may correlate with other constituents since the availability of different biomass components are relative. For example, it has been observed that abundance of cellulose correlates with abundance of lignin in five various biomass sources (Pearson's Correlation Coefficient = 0.83); similarly, presence of lignin-derived thermal products has been correlated with presence of cellulosic glucose (37). Inorganic mineral elements are no different; it has been observed that presence of Si, Al, Fe, and Na correlates with the abundance of Ti, and presence of K, P, and S correlates with Cl (36). Interactions are not only limited between cellulose and lignin constituents; GAXs (i.e. hemicellulose) in grass species have been detected to covalently link to lignin via ether bonds with ferulate esters on arabinose moieties of arabinoxylan (38). Literature suggests that xylan is the most closely linked polysaccharide to lignin, and NMR studies have backed the claim by distinguishing lignin-glucuronic acid ester bonds (39).

3.2 Relationships between biomass components and bio-oil thermal products

Pyrolysis/Torrefaction literature is indicative of how biomass constituents influence bio-oil yield upon thermal degradation of biomass. Reaction pathways and mechanisms of individual biomass components to the formation of hemicellulose, cellulose, and lignin derived thermal products have been described in detail in (40). The following discussion would focus on few "models" that help explain how different biomass constituents relate to the yield or composition of certain thermal degradation products. Figure 3.3 illustrates Model 1.
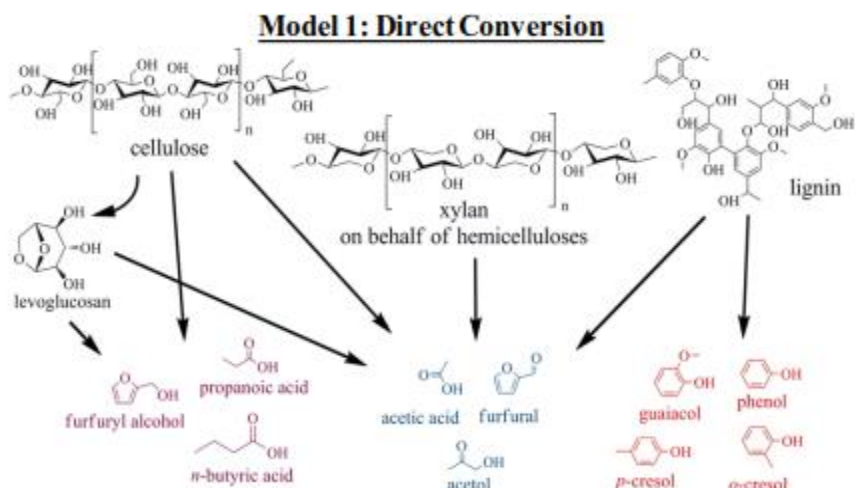
Figure 3.3: A model depicting how primary biomass components interact to form certain thermal degradation products (7)

Figure 3.3 shows how primary biomass components are direct sources of thermal degradation products. Depolymerization and secondary reactions such as cracking (i.e. splitting and recombination) allow cellulose, hemicellulose, and lignin to be converted to various products like levoglucosan, acetic acid, and phenol (among others) respectively. Evidence for the observed products as explained by this model (and other models in this chapter) are discussed below. The observations are going to be highlighted in brief detail; for all experiments performed (i.e. experiments reviewing the models presented), correlations between biomass components and thermal products have been discovered by varying starting biomass feedstock – these changes were either brought about by changing variables within experimental parameters on purified components, via naturally occurring variation within different biomass sources, or through some pre-treatment of biomass feedstock. The discussion in this thesis focuses on the chemical products produced from biomass thermal degradation (i.e. weight losses or elemental balances are not reported).

Model 1 describes the direct conversion (i.e. thermal breakdown) of the main constituents of biomass. As Figure 3.3 shows, the main product from cellulose pyrolysis is levoglucosan (41)

– an anhydrohexose that is a 1,6-anhydro-derivative of beta-D-glucopyranose; its production is maximized at 500℃ (42). Minor decomposition products from cellulose pyrolysis are generally governed by other anhydrosugars which retain the six carbons of glucose (e.g. 1,6-anhydroglucofuranose, 5-hydroxymethyl furfural); smaller molecules such as furfural (as Model 1 shows) and formic acid are also observed upon thermal degradation (43).

The type of behavior displayed by hemicellulose-derived thermal products is quite like that of cellulose-derived thermal products; both product derivatives are highly influenced by the number of carbons in the respective monosaccharide residues of the starting polymer (44). When subjected to thermal degradation, it has been detected that similar lighter compounds consisting of C_1-C_3 oxygenates are produced from pentoses and hexoses; however, heavier thermal products of C_4-C_6 oxygenates differ in their types and selectivities. It has been observed that hexoses produce more pyranic compounds upon pyrolysis than pentoses, and pentoses yield more lighter fragmentation products and less quantity of C_6 and higher products as compared to hexoses (45).

Lignin-derived thermal degradation products usually maintain the normal ring decoration of the monolignols from which they emerge; for instance, *S*-lignin monomer units produce syringol derivative bio-oil chemical compounds (Figure 3.2) while *G*-lignin monomer units form guaiacol derivative bio-oil chemical compounds (Figure 3.2). These derivative compounds contain 1-3 carbons and/or oxygenate moieties at the C-4 position (7). Grass biomass (e.g. switchgrass) has been observed to yield guaiacyl, syringyl, and p-hydroxyphenyl derivatives; in addition to these, vinyl phenol, propenyl-phenols, and p-hydroxybenzaldehyde are also produced when grasses are pyrolyzed as opposed to other species of biomass (i.e. softwood and hardwood) (37, 46). Literature suggests that these phenolic compounds are likely obtained from ferulate and coumarate esters (47). Most of the thermal products formed via lignin pyrolysis are phenol

derivatives, while trace amounts of furan derivatives and aromatic hydrocarbons are also sometimes present (46).

Another model further describes how individual components of biomass or their derived thermal products (some of which were highlighted by Model 1) facilitate the thermal reactions of other components by acting as catalysts, thereby altering thermal product yields and ratios (7). Figure 3.4 illustrates Model 2.
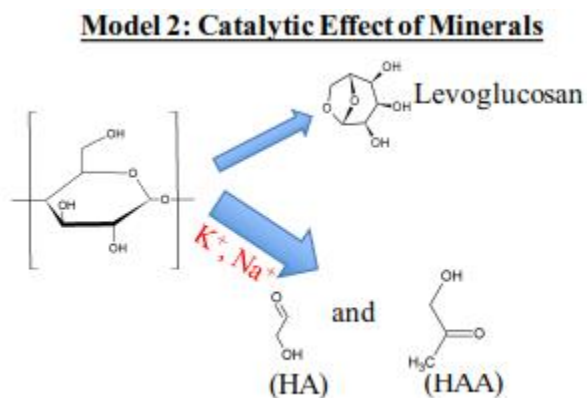
Figure 3.4: A model showing how biomass components and their interaction influence thermal degradation product formation. Here, (HA) refers to Hydroxyacetone and (HAA) refers to Hydroxyacetaldehyde (7)

Figure 3.1 lists the major biopolymers (by weight) that constitute biomass, and Model 1 established how those major constituents are primary source of bio-oil thermal products. Model 2, on the other hand, is primarily focused on the secondary reactions that take place when biomass is subjected to thermal degradation treatments; these reactions are catalyzed by the presence of other components within biomass, namely the inorganic minerals (37, 48-52). For instance, levoglucosan – a primary product of cellulose pyrolysis- has been observed to interact with the minerals present in the residual char from biomass thermal degradation to form products including, but not limited to, levoglucosenone, furan derivatives, acetic acid, acetone, and acetol.

Pretreated biomass feedstock (i.e. demineralization) decreases the formation of such substances (49,50).

Various secondary reactions are catalyzed by different mineral elements. Generally, the homolytic cleavage of pyranose ring bonds are augmented by the presence of metal cations. This augmentation comes at the expense of heterolytic cleaving of glycosidic linkages; such interaction leads to an increased formation of light oxygenate compounds and dwindles production of levoglucosan. Inorganic minerals like Na^+, K^+, Mg^{2+}, and Ca^{2+} are known to facilitate levoglucosan decomposition. However, with regards to secondary thermal products, there is a noticeable difference in the behavioral trend between group 1 alkali metals and group 2 alkali metals. Formic acid, glycoaldehyde, and acetol production has been observed to increase with increasing presence of Na^+ and K^+ than compared to similar amounts of Mg^{2+} and Ca^{2+}. However, when group 2 metal cations are in abundance compared to their respective group 1 cations, furfural production has been detected to increase. Furthermore, literature suggests that presence of alkali metals is linked to lower levoglucosan production; this is indicative of the fact that Na^+ and K^+ stimulates cracking reactions, while dehydration reactions are assisted by Mg^{2+} and Ca^{2+} (52,53). There is also evidence in literature of interactions within the polymers present in biomass indirectly affecting the conversion of thermal degradation products. Alteration of pyrolysis products due to interactions between polysaccharides and lignin are well documented in detail in (54,55). Decrease in levoglucosan yield and an increase in light (C_1-C_3) compounds (mainly glycoaldehyde and furans) have been attributed to cellulose-lignin interactions. Zhang et al. (54) have hypothesized that the cellulose-lignin interaction occupies the C_6 position which demotes the glycosidic bond cleavage required for levoglucosan formation; this change is offset by an increase in the production of lighter compounds and furans through ring scission, rearrangement,

and dehydration reactions. This phenomenon was profoundly detected in grass biomass (as opposed to other taxonomic divisions of biomass), and it coincides with the fact that grass cell walls incorporate an increased prevalence of covalent bonds between cellulose and lignin (56). Xylan-lignin interactions have also influenced pyrolysis products (7); for example, enzymatic removal of hemicelluloses from lignin-carbohydrate complexes lead to an increased coniferyl alcohol yields (55).

While years of research have improved understanding of how monomeric and polymeric units of biomass lead to thermal products, including the significance of catalytic degradation, detailed comprehension in the correlation of biomass components and their respective related products is an area that can be further explored upon. Biological literature is continuously updating details on the characterization of cell wall components, while engineering literature continues to assess the chemical components (i.e. yields) of different pyrolytic fragments. It is reasonable to argue that more comprehensive relationship studies between biomass components and thermal degradation products will allow for more refined product quality since up-grading strategies are heavily influenced by bio-oil composition.

Generally, upgrading strategies are better facilitated with simpler and distinguished thermal product streams if C-C bonds and overall C-content are still maintained. To get a more thorough explanation of biomass-bio-oil relationship, more sophisticated analysis of biomass composition and thermal degradation products within species of the same biomass that display compositional variation is required. Much of the understanding and comparison within such a relationship in literature is based on biomass across different taxonomic divisions (i.e. softwood, hardwood, grass biomass). An analysis of slightly more rigorous difference across the same type of biomass where compositional factors are varied is the focus of this thesis. For instance, genetic

mutations leading (ideally) to a variance of only one component as compared to unmutated "wild type" plant of the same species can directly assess a more comprehensive relationship between starting feedstock and its relative products (7).

Apart from selecting or breeding for natural variation within the same species of a specific biomass, genetic modification to target specific variation in biomass composition is an area that is quite compelling. In simple terminology, genetic engineering of bioenergy plants can be attained by altering the plant's genome to do either of the following: expressing genes from other organisms, increasing the expression of native genes, or reducing the expression of native genes (7). The motive behind genetically maneuvering biomass feedstock composition is to either increase the yield of favorable bio-oil thermal products or to decrease the yield of unfavorable bio-oil thermal products in order to simplify (i.e. economically favorable) up-grading strategies. The foundation in genetically engineered bioenergy crops is based on the following concepts: comprehension of the biosynthetic pathway of cell wall formation including the individual genes culpable for the formation of major polymer units and the covalent interactions among them (7,26,57), regulation of the biosynthetic cell wall gene expression (58), and navigation of metal ion transport proteins which influence the relative abundance of inorganic mineral elements within plant species (59,60). Lignin, for instance, is a notable target for genetic modification – an area which this thesis will focus on in the following chapter- since lignin-derived thermal degradation products tend to have a lower O:C ratio and a higher energy value than sugar-derived thermal degradation products (7).

Apart from genetic modification, pre-treatment of biomass species is another strategy that is used to improve the quality of biomass by altering biomass composition for simpler and more refined thermal product streams. One such pre-treatment strategy is torrefaction; it is a low

temperature (200-400 ℃) thermal decomposition process that removes most of the hemicellulose and separates unfavorable products such as water and acids into intermediate streams before the next stage of thermal degradation treatment can be applied (61). Torrefaction – in conjunction with genetically modified biomass- may help alter the biomass composition to a greater degree resulting in a more refined thermal segregation (i.e. hemicellulose decomposition could be completely separated (or maximized) from a stream containing decomposition products from cellulose and lignin). This could be achieved by detecting and understanding the roles played by various crucial biomass components- specifically in the lignin biosynthesis network- to maximize economical benefits of plant derived biofuels.

3.3 Selection of temperature and time parameters for Torrefaction/Pyrolysis

As mentioned in Chapter 1, the thermal stability regimes of cellulose and lignin overlap quite a bit; thus, achieving a thermal product stream devoid of hemicellulose-derived products and encompassing more of the cellulose-derived and lignin-derived products (e.g. levoglucosan and the phenolic substances) is of interest. It is crucial to keep in mind that the overwhelming focus of this thesis is eliminating lignin-derived products from the first stage (primarily hemicellulose) torrefaction stream.   Analytical pyrolysis determines the thermal product composition which results from both time and temperature variation. Standard grade AP 13 switchgrass biomass (obtained from the Microbiology department at The University of Oklahoma) were utilized for torrefaction experiments as a precursor step to pyrolysis to identify relevant chemical compounds and compound groups.

Hemicellulose has the lowest thermal degradation temperature range amongst the 3 major polymeric components of biomass; it has a lower decomposition temperature than cellulose while lignin has the broadest thermal degradation temperature change. Considering this, and the fact

that the residence time of the thermal degradation unit employed did not exceed 2 minutes for any experiments, it was decided that torrefaction of AP13 switchgrass would be evaluated at 290 ℃. Previous work on oak biomass had been carried out at this temperature, even though the reactor used and residence time employed were different (6,7). This was also taken into consideration when choosing initial conditions for AP 13 switchgrass experiments. Furthermore, it has been determined that temperatures between 500℃ - 550℃ is efficient for fast pyrolysis of biomass to optimize overall liquid yield (62).

Three technical replicates of the same mesh size of AP13 switchgrass were, therefore, torrefied at 290℃ for 120 seconds followed by pyrolysis at 500℃ for 60 seconds. A blank tube in between each switchgrass sample was placed for cleaning any residual vapors from previous experimental runs at a temperature of 1000℃. To regulate minimal thermal gradient for a uniform torrefaction/pyrolysis process, the sample sizes for these technical replicates – and the subsequent samples included in this section of the thesis- were kept relatively small (i.e. varied from about 0.50 mg to around 2.20 mg). Each identified chemical compound was then lumped into the following organic groups: Light Oxygenates, Acetic Acid, Furfurals, Furans, Alkyl Benzenes, Alkyl Phenols, Anhydrous Sugars, and Methoxy Phenols. Figure 3.5 and Figure 3.6 depict the composition of the different product streams resulting from the thermal degradation of AP 13 switchgrass. Evaluation of 290 degrees torrefaction were not satisfactory due to extremely low pyrolytic yields, as evidenced by Figure 3.6.
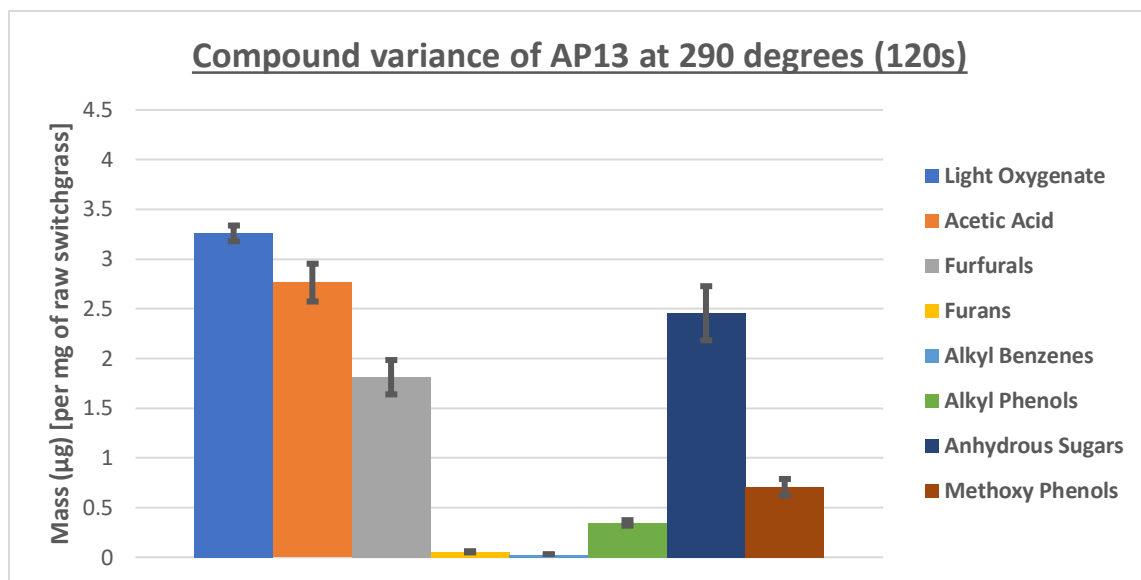
Figure 3.5: Yield showing different composition streams of AP13 Switchgrass upon torrefaction with a residence time of 120 seconds

Figure 3.6: Yield showing different composition streams of torrefied AP13 Switchgrass upon pyrolysis with a residence time of 60 seconds

While torrefaction of the AP13 switchgrass shows variation in the composition of thermal product streams (i.e. thermochemical products of each compound lump being produced), Figure 3.6 displays barely any product upon pyrolysis. With the aim of torrefaction being removal of hemicellulose-derived thermal products to attain a subsequent pyrolysis stream comprising mainly cellulose-derived and lignin-derived products, the treatment of torrefaction (i.e. temperature) seems harsh (i.e. low pyrolytic yields). The abundance of anhydrous sugars in Figure 3.5 is due to levoglucosan – a primary product of cellulose pyrolysis; this, in association with the presence of the phenolic species upon torrefaction and absence of the phenolics during pyrolysis of the torrefied biomass, further reiterated that temperature and time parameters for the thermal treatments would need to be altered. The aim was to find conditions which would allow a proper assessment of the influences of biomass genetic modification on thermal products of torrefaction and pyrolysis. Reduction of the residence time of torrefaction to 60 seconds still yielded more anhydrous sugars and phenolics than their respective amounts during pyrolysis (as Figure 3.7 and Figure 3.8 determines).
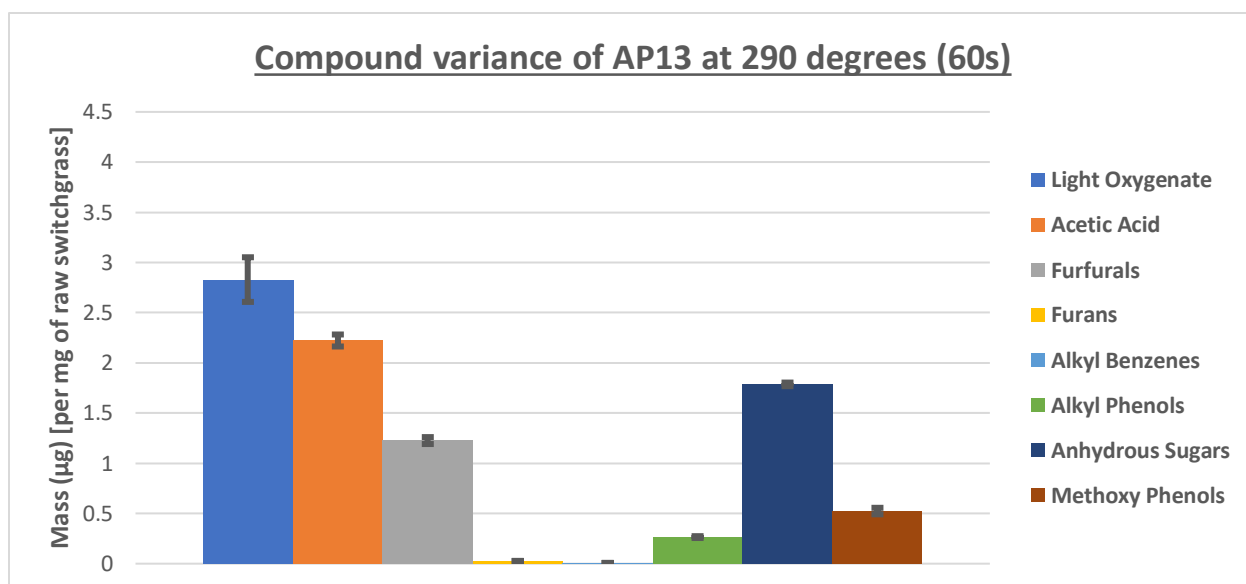
Figure 3.7: Yield showing different composition streams of AP13 Switchgrass upon torrefaction with a residence time of 60 seconds

Figure 3.8: Yield showing different composition streams of torrefied AP13 switchgrass upon pyrolysis with a residence time of 60 seconds

Figures 3.5- Figures 3.8 helped establish that the temperature treatment for torrefaction of the biomass was too severe since subsequent pyrolysis of the torrefied biomass at 500 ℃ failed to produce expected relative quantity of chemical compounds. These experiments were conclusive of the fact that enough biomass was not left within the sample tube for adequate pyrolysis. In addition to this, literature pointed out that cellulose has been seen not to undergo significant mass loss at temperatures under 275 ℃ (63). Consequently, a 270 degrees torrefaction with a residence time of 120 seconds followed by pyrolysis at 500 degrees for 60 seconds showcased thermal product compositional segregation across all compound lumps during both thermal treatments. The results, which are displayed in Figure 3.9 and Figure 3.10, were convincing of the fact that such employed experimental parameters (temperature and time) would provide a situation where the effects of heritable traits on low temperature thermal treatments can be evaluated. Moreover, Figure 3.11 and Figure 3.12 highlight good quantitative and qualitative reproducibility – with the exception of acetic acid- across all compound groups for the same thermal degradation conditions.
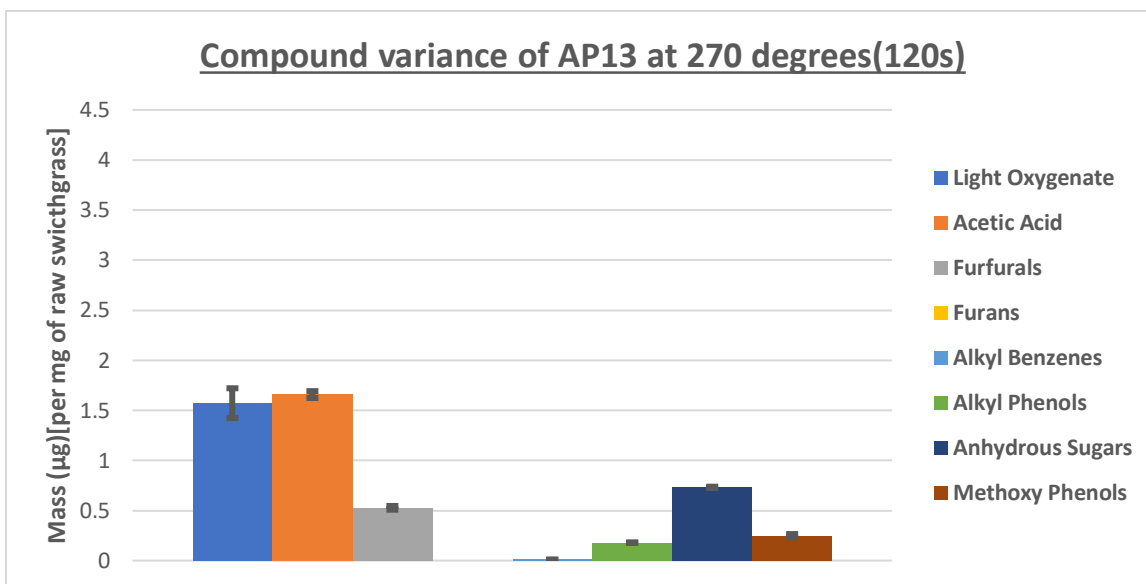
Figure 3.9: Yield showing different composition streams of AP13 Switchgrass upon torrefaction at 270 degrees Celsius with a residence time of 120 seconds
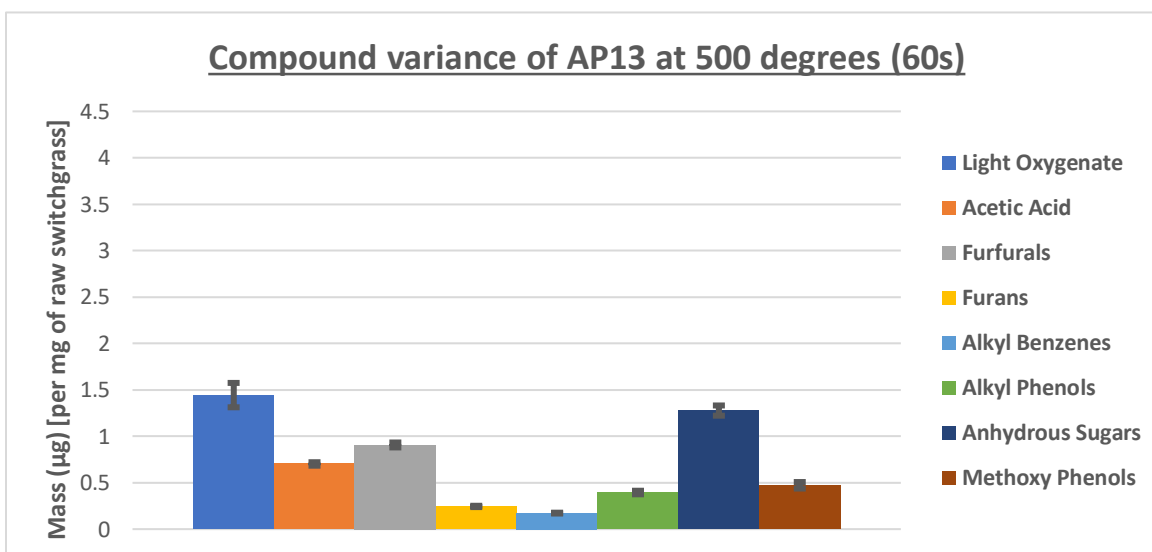
Figure 3.10: Yield showing different composition streams of torrefied AP13 Switchgrass upon pyrolysis with a residence time of 60 seconds

At these lower temperatures of torrefaction, as expected, lesser amounts of all organic compounds are produced due to the biomass being degraded to a lesser extent. Of particular interest is the amount of anhydrous sugars being produced at 270 ℃ , which is approximately 41% of the amount being produced at 290 ℃ with a residence time of 60 seconds and approximately 30% of the amount being produced at 290 ℃ with a residence time of 120 seconds. However, it is seen that yield of anhydrous sugars increases upon pyrolysis of the torrefied biomass – a phenomenon not seen at the higher temperature pyrolytic thermal treatments with either residence times. The selectivity towards phenolic species upon torrefaction decreased as well- less than half of what was being observed at 290 ℃ for 120 seconds; however, the selectivity increased once the torrefied biomass was pyrolyzed (which was not being observed at higher torrefaction temperatures).
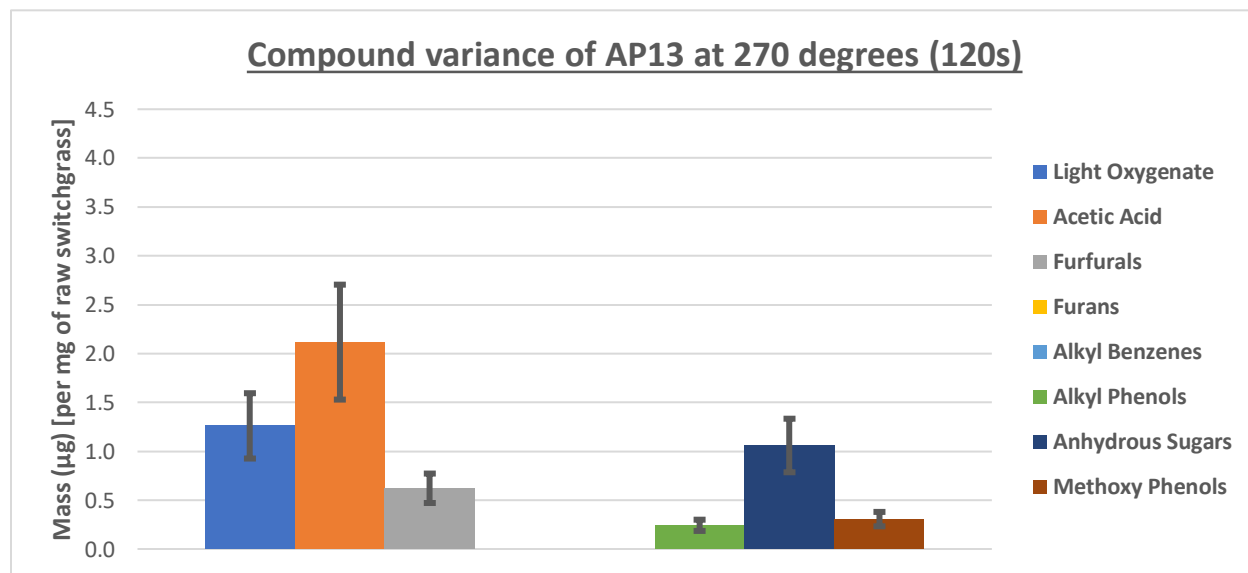
Figure 3.11: Yield showing different composition streams of AP13 Switchgrass upon torrefaction at 270 degrees Celsius with a residence time of 120 seconds
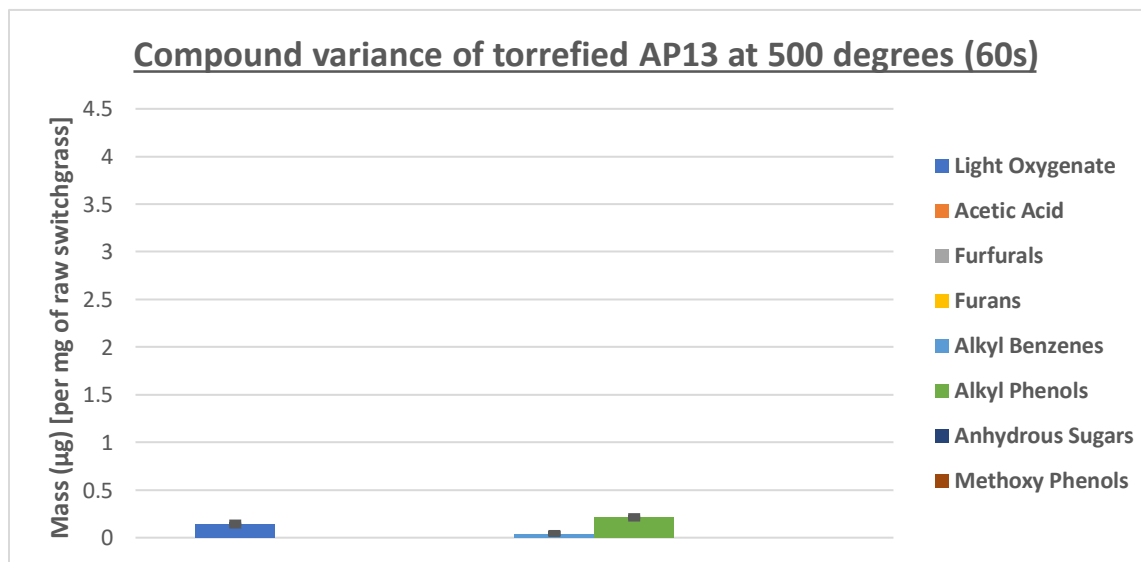
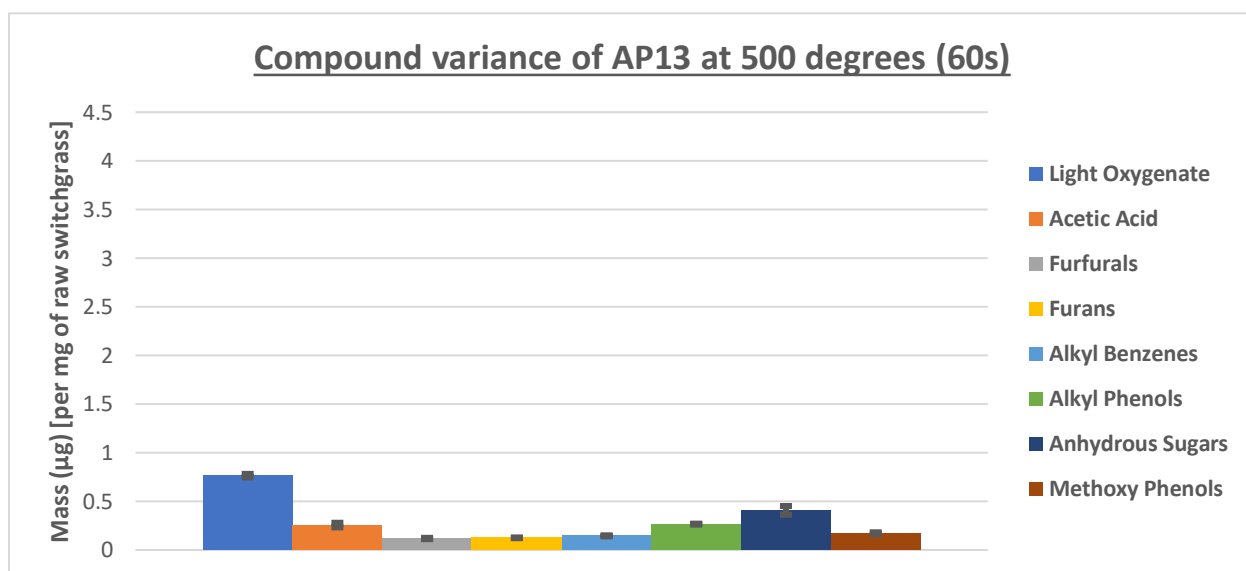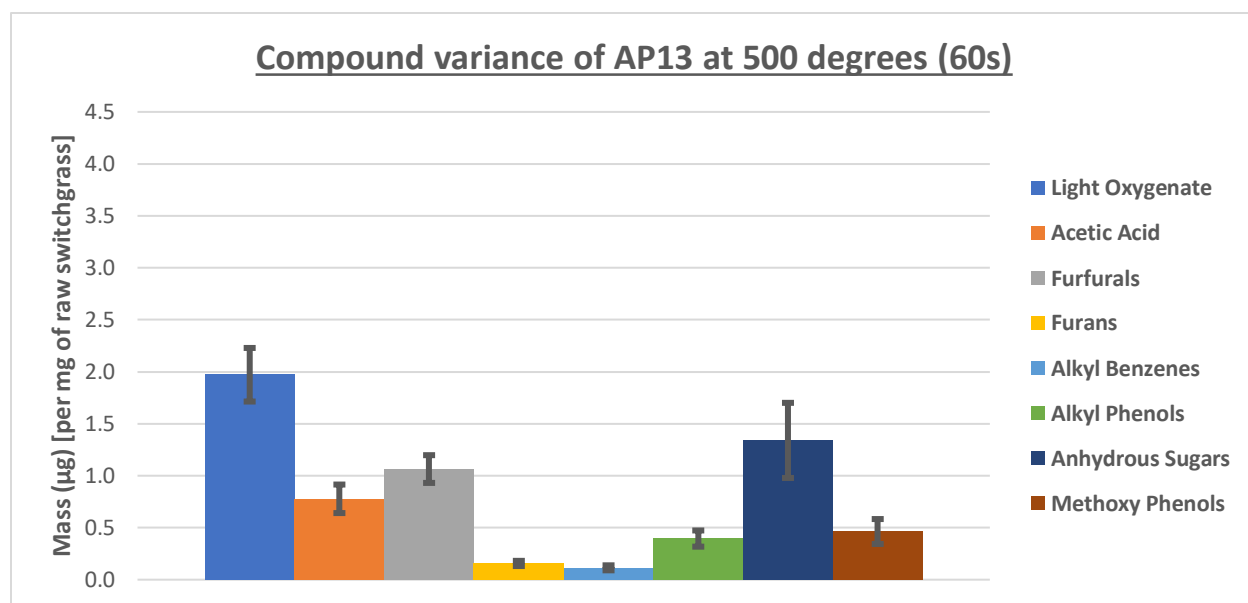**Figure 3.12**: Yield showing different composition streams of torrefied AP13 Switchgrass upon pyrolysis with a residence time of 60 seconds

Chapter 4 : The effect of genetic modification of lignin biosynthesis pathway on torrefaction product yields

Parts of this chapter has been extracted from a manuscript in preparation

Redwan Nazim, Fan Lin, Christopher Waters, Rajiv Janupala, Richard Mallinson, Laura Bartley, Lance Lobban

4.1 Introduction

The results of previous chapter provide evidence that temperature and residence time provide means to exercise influence over the thermochemical degradation products. Previous studies have shown the different segregation of thermochemical products through the manipulation of process variables (6,7); this allows for various catalytic valorization techniques to be customized to each separate product stream to maximize desirable output (i.e. maximizing carbon yield, enhancing process economics, etc.). A desirable objective of this thesis is to determine/pinpoint which different organisms/compositional factors (i.e. by investigating the heritable traits) are responsible for different thermochemical products within a single species of biomass (in this case, switchgrass).

As mentioned briefly in Chapter 1, a desirable segregation is the "clean" removal of hemicellulose through a low-temperature thermal degradation treatment (i.e. a treatment that would minimize cellulose and lignin decomposition as much as possible while degrading almost all of hemicellulose). Preceding studies, though, have detected small amounts of cellulose and lignin decomposition at low temperature treatments (7). While cellulose degradation can be minimized (as evidenced by the absence of levoglucosan in the 270 degrees torrefaction result in previous chapter), literature suggests that some lignin decomposition would always take place at

conditions which degrade hemicellulose (9,64) due to lignin's broad thermal stability range (shown in chapter 1).

Utilizing a biomass feedstock with a low lignin content might help address the objective of minimizing lignin-derived thermal products to a greater extent, although high amounts of such thermochemical conversion products, especially the phenolic species, are sought after from the whole thermal treatment procedure. Considering such factors, adapting the thermal stability region of lignin to suppress its decomposition at lower temperatures without affecting the total lignin content present within the biomass species would allow both outcomes (i.e. degrading hemicellulose completely and minimizing lignin decomposition via low temperature thermal treatment) to come to fruition.

4.2 Lignin Biosynthesis Network

As discussed in Chapter 3, lignin is a class of complex organic polymers consisting primarily of 3 monomeric units (*H*, *G*, and *S*) that compose key framework materials in the support tissues of vascular plants (i.e. cell walls) (29); an overview of these monomeric units (which is our primary focus) and their resulting structures (included by author for completeness) in the polymer is provided in Figure 4.1 (29). It is due to the prevalence of so many different linkages within the lignin polymeric network that attributes for such a broad range in its thermal stability. Amongst all the structures shown in Figure 4.1, the most commonly occurring unit within the lignin biosynthesis network is the β-O-4 structure – it incorporates more than half of the inter-unit linkages within the network (29). Apart from this structure, other frequently occurring units are β-5, β-β, 5-5, 5-O-4, and β-1 structures.
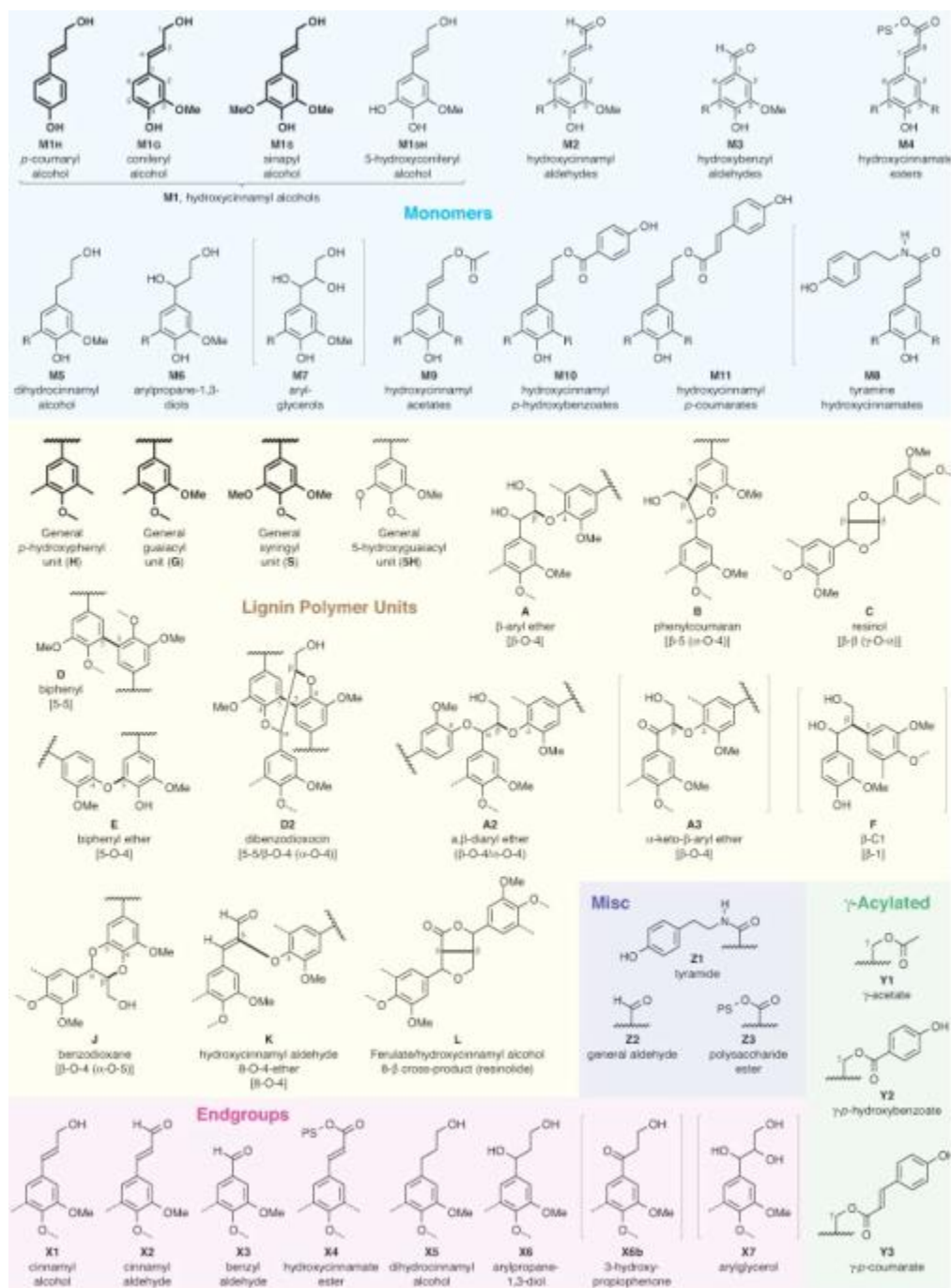
Figure 4.1: Lignin monomers and structures within the polymer; lignins derive primarily from three monolignols – the hydroxycinnamyl alcohols: M1H, M1G, and M1S (29)

For the six structures mentioned within the biopolymeric lignin network, DFT calculations measuring the enthalpy of dissociation for these six bonds were carried out; the findings are provided in Figure 4.2 (7). Literature suggests a correlation that an increase in the production of *G* monomeric units over *S* monomeric units (i.e. in other words, a lower *S/G* ratio) results in an increased pervasiveness of β-5, 5-5, and 5-O-4 structures over β-O-4, β-β, and β-1 linkages within the lignin polymeric network; this correlation has been attributed to the increased availability of the "5" position as a reaction site (29). This finding is explained in detail in (29). In accordance with this, and the DFT measurements, it is reasonable to state that commencement of the radical depolymerization reactions within the lignin biopolymeric network would be less favorable (i.e. as it requires greater energy for bond dissociation) at lower temperature thermal treatment for biomass species exhibiting lower *S/G* ratios. As a result, selectivity for lignin decomposition at the lower temperature thermal treatment would decrease.
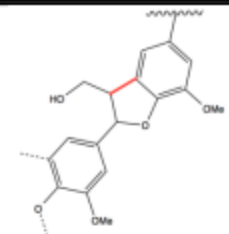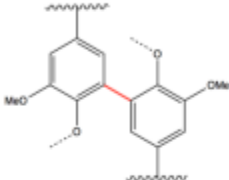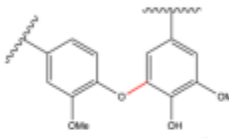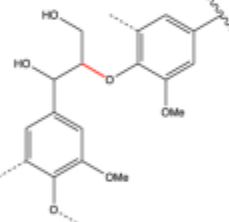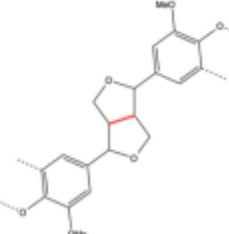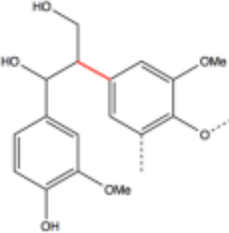
Bond	Structure	ΔH_{diss}, kcal/mol, 298K
β-5		101.6 – 107.1
5-5		111.8 – 118.1
5-O-4		77.7 – 82.5
β–O–4		67.7 – 71.3
β-β		81.1 – 82.6
β-1		64.7 – 69.1

Figure 4.2: Enthalpy of dissociation measurements for the six most frequently occurring lignin crosslinks (7)

Figure 4.3: Monolignol and Phenylpropanoid biosynthetic pathways with the enzymes responsible for multiple steps (29)

Lignin synthesis is a biological process which includes numerous steps for the production of the three primary monolignols. (29) demonstrates how lignin's synthesis could be impacted by heritable traits. Several enzymes determine lignin biosynthesis which is illustrated in Figure 4.3

(it displays how numerous enzymatic actions are involved in the phenylpropanoid synthesis pathway) (29). One of the enzymes – Caffeic acid O-methyltransferase (COMT)- is responsible for the production of sinapaldehyde and sinapyl alcohol via the methylation on 5-OH group. Sinapaldehyde and sinapyl alcohol act as precursors of the *S* lignin monomer. The genetic modification done on the biomass (i.e. switchgrass) used in this study downregulates the production of COMT enzyme. As a result, the *S/G* ratio in the lignin network of the genetically modified biomass is lowered. This thesis hypothesizes that such a modification to the lignin biosynthesis network would result in lower phenolic product yields in the downregulated COMT deficient mutant switchgrasses as compared to their unmodified wild type switchgrass when subjected to a low temperature thermal degradation treatment (i.e. torrefaction).

4.3 Experimental

C. N. Stewart and associates, in conjunction with the Microbiology department at The University of Oklahoma, provided dry switchgrass biomass of an independent Caffeic acid O-methyltransferase knock down line (COMT2); detail explanation of the process and characteristics of the biomass is described in Baxter et al. (65). The COMT2 mutant variants and their respective isogenic wild type switchgrass samples portray significant differences in their *S/G* ratios (measurement of this ratio for the mutants were around 0.45 while the wild types were over 0.7); the samples chosen only exhibited slight differences in the total lignin content (i.e. mutants lower than the wild types) while all other contents within the biomass were relatively similar. This was ensured in an attempt to closely attribute the compositional differences in the yield of the thermal products to the genetic modification (rather than any other influencing factors present in the switchgrass).

The dry switchgrass used for the thermal degradation experiments was ground utilizing a Thomas Wiley Mini-Mill with a 60-mesh screen. Approximately 10 mg of each variant (i.e. mutant and wild type) of the COMT2 switchgrass was provided. From this pool, samples weighing approximately between 0.75-1.50 mg was prepared for analysis in a CDS Analytical 5250T pyroprobe, in conjunction with a Shimadzu QP-2010+GC/MS-FID system. Sample preparation and analytical techniques have been described in Chapter 2. The identified compounds and their lumps as used for the analysis of the studies within this thesis is provided in Table 1 in the appendix.

In addition to the torrefaction/pyrolysis of the COMT2 mutant and isogenic wild type switchgrasses, standard grade AP13 and natural diversity switchgrass samples (both provided by the microbiology department at The University of Oklahoma) were also subjected to identical thermal treatments; the AP13 and natural diversity switchgrasses help establish reference points for the comparisons being made. It is crucial to note that the natural diversity switchgrass samples exhibit low *S/G* ratio (common characteristic with the COMT2 mutant) while the standard AP13 exhibit high *S/G* ratio (common characteristic with the COMT2 wild type). Differences that may be observed upon the analysis of results among only the COMT2 variants could be attributed to the changes caused by the genetic modification since the specific genetic modification made is the only difference between the contents of the COMT2 switchgrass samples. However, some trends observed in the thermochemical products of the other two samples (e.g. similarities and differences) cannot be guaranteed to be a result of a single change due to other differences/similarities present within those biomass samples – the *S/G* ratio is only one characteristic that is common between the COMT2 variants and the other biomass samples. The AP13 and natural diversity samples chosen had no deliberate control/influence on their lignin

biosynthesis pathway. Hence, they are interesting choices (due to their similarities in the S/G ratio with each variant of the COMT2 switchgrass) as reference points for the comparisons to be made upon analysis of the thermal degradation treatments (i.e. to study the effects of the influence of the differences in *S/G* ratio at low temperature torrefaction). It is expected that phenolic yield in samples with low *S/G* ratio will be less than the yield in samples with high *S/G* ratio, although the extent of thermochemical product conversion is unclear due to natural variances within the AP13 and natural diversity samples potentially affecting biomass conversion.

4.4 Results

The four different variants of switchgrass were torrefied at 270 ℃ with a residence time of 120 seconds; the torrefied biomass was then pyrolyzed at 500 ℃ for 60 seconds. The thermochemical products (in compound lumps) from the four samples run are shown in Figure 4.4 and Figure 4.5 respectively. Table 4.1 and Table 4.2 quantifies the yield of the compound lumps per milligram of the raw biomass; Figure 4.6 and Figure 4.7 separately shows the yield of the phenolic species (both alkyl and phenolic) upon torrefaction and pyrolysis respectively, while Figure 4.8 lists the phenolic species that have been identified in this study. The error bars shown in the figures represent the standard deviation of three triplicate samples of biomass torrefied/pyrolyzed consecutively.
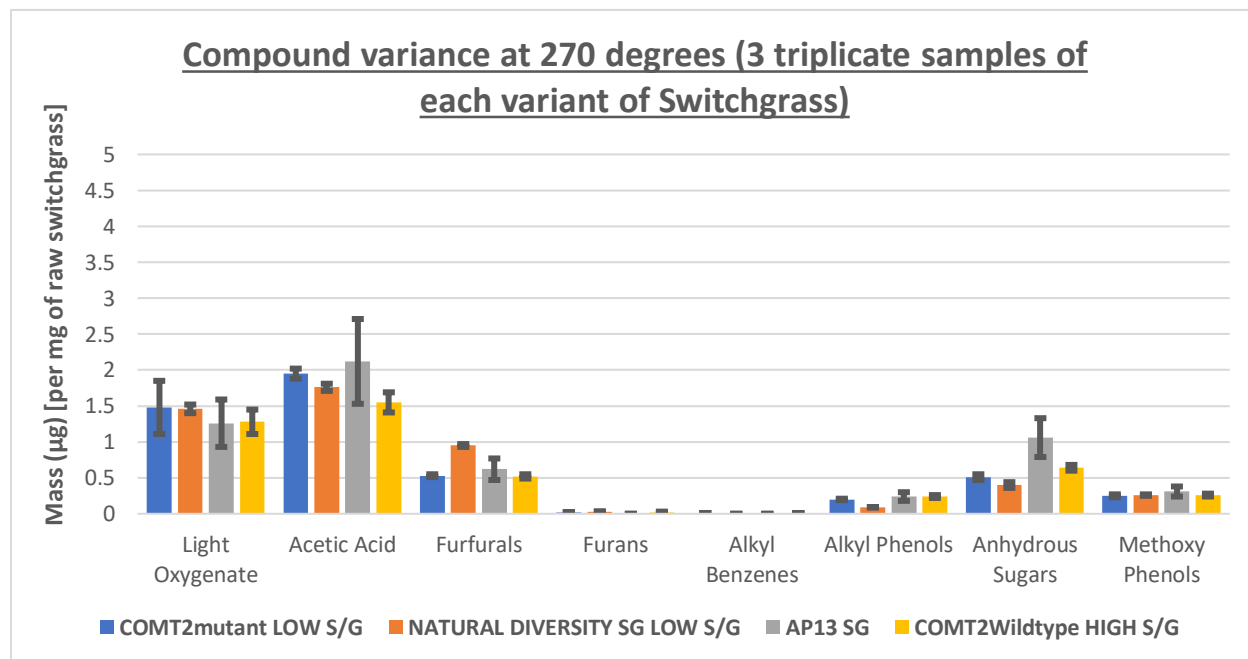
Figure 4.4: Compound yield of different variants of switchgrass upon torrefaction at 270 degrees Celsius for 120 seconds
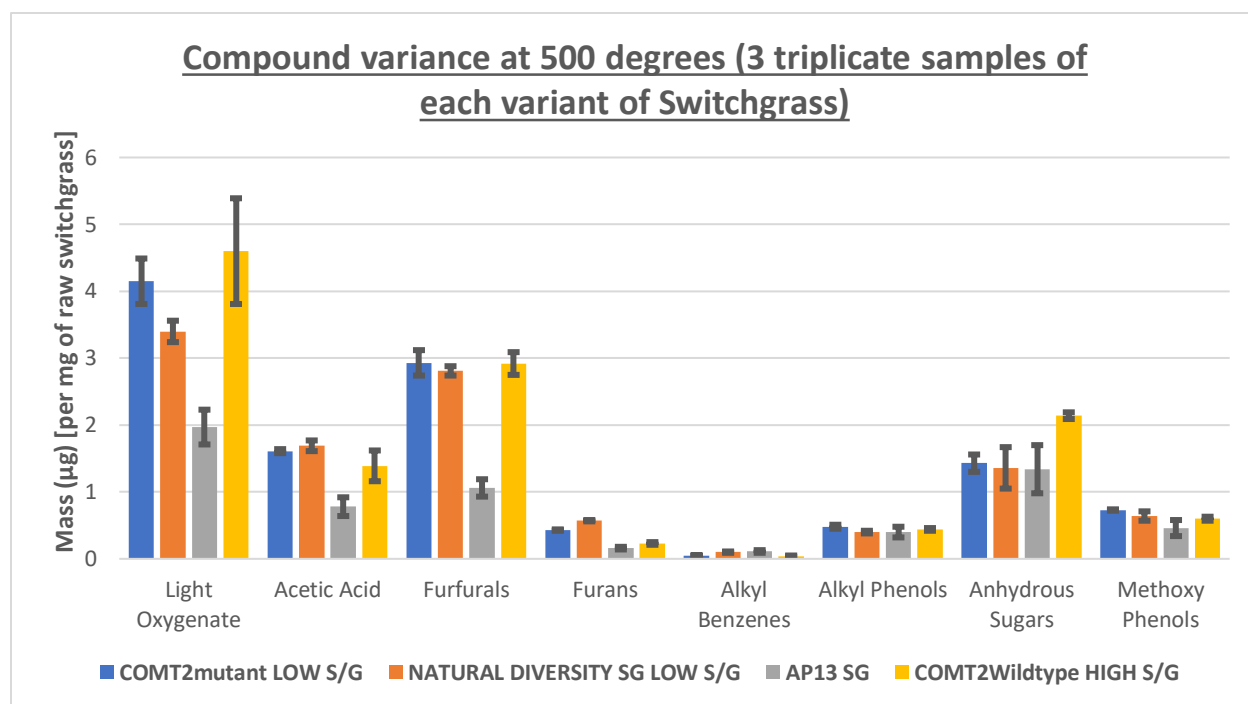
Figure 4.5: Compound yield of different variants of switchgrass upon pyrolysis at 500 degrees Celsius for 60 seconds

Table 4.1: Torrefaction yield of different compound lumps per milligram of raw biomass

Torrefaction yields of different variants of switchgrass per milligram of biomass									
		Light Oxygenate	Acetic Acid	Furfurals	Furans	Alkyl Benzenes	Alkyl Phenols	Anhydrous Sugars	Methoxy Phenols	**Total**
Mass (µg)	COMT2mutant	1.48	1.95	0.53	0.02	0.01	0.2	0.51	0.25	**4.95**
	NATURAL DIVERSITY SG	1.46	1.76	0.95	0.03	0	0.09	0.4	0.26	**4.95**
	AP13 SG	1.26	2.12	0.62	0	0	0.24	1.06	0.31	**5.61**
	COMT2Wildtype	1.28	1.55	0.52	0.02	0.01	0.24	0.64	0.26	**4.52**

Table 4.2: Pyrolysis yield of different compound lumps per milligram of raw biomass

Pyrolysis yields of different variants of switchgrass per milligram of biomass									
		Light Oxygenate	Acetic Acid	Furfurals	Furans	Alkyl Benzenes	Alkyl Phenols	Anhydrous Sugars	Methoxy Phenols	**Total**
Mass (µg)	COMT2mutant	4.15	1.61	2.93	0.43	0.05	0.48	1.43	0.73	**11.81**
	NATURAL DIVERSITY SG	3.4	1.69	2.81	0.57	0.1	0.4	1.36	0.64	**10.97**
	AP13 SG	1.97	0.78	1.06	0.16	0.11	0.4	1.34	0.46	**6.28**
	COMT2Wildtype	4.6	1.39	2.92	0.23	0.04	0.44	2.14	0.6	**12.36**
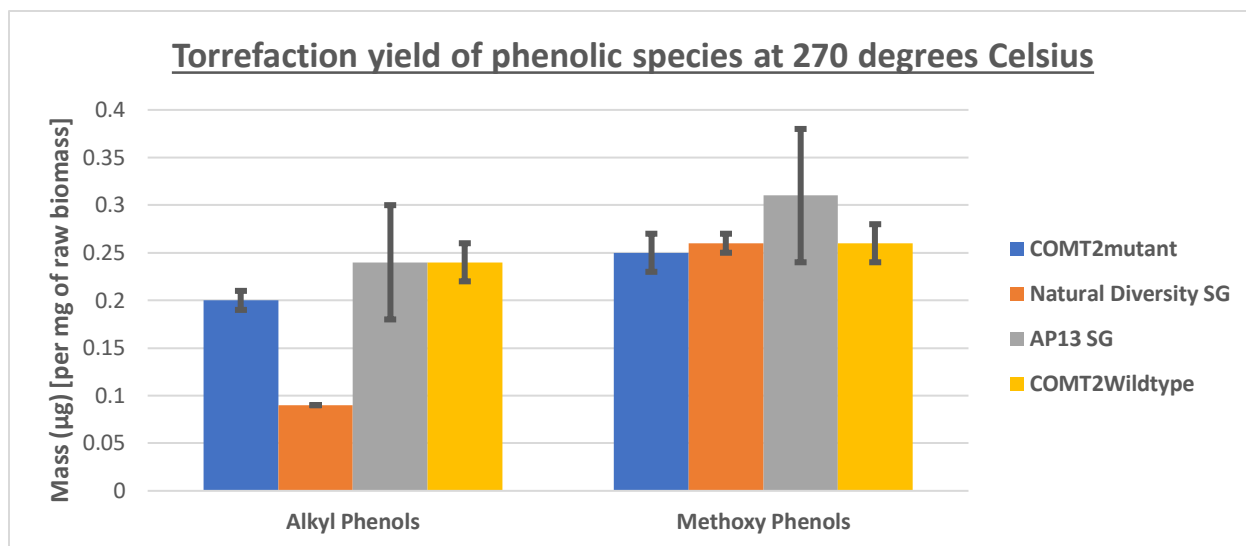
Figure 4.6: Yield of the phenolic species upon torrefaction of different variants of switchgrass
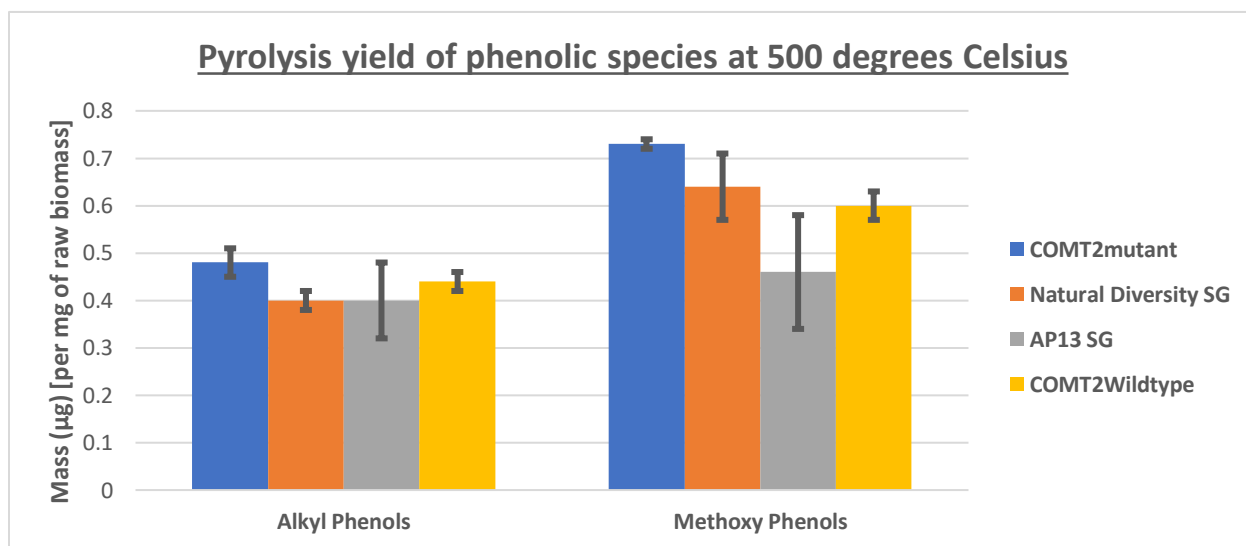
Figure 4.7: Yield of phenolic species upon pyrolysis of different variants of switchgrass

<div style="border:1px solid black; padding:1em;">

<u>Alkyl Phenols:</u>

Acetophenone
m-Cresol
p-Cresol
o-Cresol
Phenol
Phenol,2-ethyl-
Phenol,4-vinyl-
Catechol
Catechol,4-methyl-

<u>Methoxy Phenols:</u>

Guaiacol
Guaiacol,3-methyl-
Guaiacol,4-ethyl-
Guaiacol,4-vinyl-
Eugenol
Isoeugenol (cis/trans)
Syringol
Syringol,4-methyl-
Syringol,4-ethyl-
Syringol,4-vinyl-
Syringol,4-propenyl-
(cis/trans)
Acetoguaiacone
Vanillin
Homovanillin
Coniferaldehyde

</div>

Figure 4.8: List of phenolic compounds identified during analysis of thermal degradation experiments for this study

Looking at the compound lumps of the torrefaction results, the hypothesis that the genetic modification performed on the mutant switchgrasses would lead to lower phenolic yields at the low temperature thermal degradation treatment as compared to their unmodified, isogenic wild type switchgrass holds true. However, looking at Figure 4.4 and Table 4.1, it is evident that the difference is more pronounced in the alkyl phenolic yields as opposed to methoxy phenol yields (although it is important to note that mutant methoxy phenol yields are still less than the wild type methoxy phenol yields).The COMT2 mutant produces 0.2 µg of alkyl phenols and 0.25 µg of methoxy phenols, while the COMT2 wild type produces 0.24 µg of alkyl phenols and 0.26 µg of methoxy phenols. The lowest alkyl phenolic yield amongst all the variants was exhibited by the natural diversity switchgrass sample (0.09 µg) – which has a low *S/G* ratio. A speculation of why such is the case in the natural diversity sample may be attributed to the samples containing lowered levels of p-Coumaric acid (pCA) (66). The basis behind this speculation lies in the observed 23% increase in the production of Guaiacol,4-vinyl- (a product of esterified ferulic acid) when compared to its yield through the COMT2 mutant switchgrass. Details as to how lowered levels of pCA may contribute to lower phenolic yields at low temperatures is debated in the discussion section below. Even though natural diversity exhibits similar *S/G* ratio to the COMT2 mutant sample, the alkyl phenolic yield of COMT2 mutant (0.20 µg) is more than double of the natural diversity sample. The µg numbers reported are in the basis of per mg of raw biomass. In addition to this, the AP13 switchgrass sample had an identical alkyl phenolic yield to the COMT2 isogenic wild type switchgrass- both of which have high *S/G* ratio.

Comparable amounts of methoxy phenols (per mg of raw biomass) were produced across all variants of switchgrass when subjected to torrefaction conditions. The methoxy phenol yield of the COMT2 mutant (0.25 µg) was less than that of the COMT2 wild type (0.26 µg) – however,

the difference is almost negligible. It is also notable that the natural diversity switchgrass sample (low *S/G* ratio) had an identical methoxy phenol yield to the COMT2 wild type sample (high *S/G* ratio); this ties back to the point made earlier that other factors within the contents of the biomass could also influence thermochemical product yields. The highest methoxy phenol yield upon torrefaction was observed in the standard AP13 grade sample (0.31 µg). The µg numbers reported are on the basis of per mg of raw biomass.

Reproducible amounts of other compound lumps were observed across all four variants of switchgrass samples upon torrefaction with a few exceptions; the natural diversity switchgrass sample produced almost double the amount of furfurals compared to the other three variants of switchgrass, while AP13 also produced almost double the amount of anhydrous sugars compared to the other three switchgrass samples. Table 4.1 shows the raw numbers of these observations. The anhydrous sugars detected in all the torrefaction switchgrass samples are hemicellulose-derived thermal products since no levoglucosan – a primary product of cellulose pyrolysis- was identified in any of the samples.

Looking at Figure 4.5 and Table 4.2, the pyrolysis trends are more erratic when compared to torrefaction trends. It is reasonable to state that the thermal treatment of the torrefied biomass at 500 ℃ for 60 seconds leads to a rapid and near-complete conversion of the switchgrass samples. The degree of torrefaction decomposition seems to be the highest on AP13 switchgrass sample as it produced the least number of thermochemical products across all compound lumps upon pyrolysis – with the exception of anhydrous sugars and alkyl benzenes (whose thermochemical products are almost negligible anyway). The COMT2 mutant and natural diversity switchgrass – both exhibiting low *S/G* ratio- produces reproducible amounts of thermochemical products across

all compound lumps. The isogenic COMT2 wild type switchgrass produces the most thermochemical products across all compound lumps upon pyrolysis.

Quantitatively, both the phenolic species produced greater numbers upon pyrolysis than torrefaction across all four variants of switchgrass samples – which is a rational expectation of lignin-derived phenolics to be decomposed to a larger extent with the rise in temperature treatment. Considering only the COMT2 variants of switchgrass samples, the combined total yield of alkyl phenolic species per mg of raw biomass upon torrefaction and pyrolysis is 0.68 μg for both the mutant and wild type sample. However, according to Table 4.1 and Table 4.2, the difference in their yields from torrefaction to pyrolysis is greater in the COMT2 mutant than in the COMT2 wild type switchgrass (the mutant produces 0.2 µg in torrefaction and 0.48 µg in pyrolysis, while the wild type produces 0.24 µg in torrefaction and 0.44 µg in pyrolysis). In addition to this, the combined total yield of phenolic species (both alkyl and methoxy) per mg of raw biomass upon torrefaction and pyrolysis is 1.66 µg for the mutant sample and 1.54 µg for the wild type sample; while producing less phenolics during torrefaction, it is observed that the mutants had a 7.5% increase phenolic production from the overall thermal degradation treatment (i.e. torrefaction followed by pyrolysis). This observation – lower phenolics yield for the COMT2 mutants as opposed to their respective wild types due to a suppression of lignin decomposition at low temperature thermal treatment without altering the total lignin content present within the biomass sample- is a positive reinforcement of the hypothesis made, and can be attributed to the changes caused by the genetic modification.

The natural diversity switchgrass (low *S/G* ratio) and the standard AP13 (high *S/G* ratio) had an identical alkyl phenolic yield upon pyrolysis, but the natural diversity sample produced a greater amount of methoxy phenols than the AP13. In addition to this, Table 4.1 and Table 4.2

indicate that the low *S/G* ratio sample produced less phenolics (both alkyl phenols and methoxy phenols combined) than the high *S/G* ratio sample (0.35 μg for natural diversity sample compared to 0.55 μg for AP13) at the low temperature treatment while the total combined phenolic yields upon torrefaction and pyrolysis is almost the same (1.39 μg for the natural diversity sample as compared to 1.41 μg for the AP13 switchgrass). Even though there are other compositional factors that are different within these two specific species of switchgrass (other than the differences in their *S/G* ratio) – which may contribute for the same alkyl phenolic yield (0.4 μg) of pyrolysis, the observed total phenolic yields upon subsequent thermal treatments help to establish reference points as a positive indicator of the hypothesis made in this thesis. The μg numbers reported are on the basis of per mg of raw biomass.

Figures 4.10-4.13 display the distribution of *S*-lignin derived and *G*-lignin derived products amongst the identified phenolic species (considering both alkyl phenols and methoxy phenols) upon torrefaction and pyrolysis of the COMT2 variants of switchgrass. Figure 4.9 lists the individual identified phenolic compounds through their originating monomer unit. Considering torrefaction analysis (Figure 4.10 and Figure 4.11) between the COMT2 variants, the results are dominated by Guaiacol,4-vinyl- (*G* monomer derived) as it constitutes approximately 45% and 56% of the *G*-lignin derived phenolic products for the mutant (low *S/G* ratio) and wild type sample (high *S/G* ratio) respectively. While it is expected that the wild type sample has a greater percentage of Guaiacol,4-vinyl- due to the increased abundance of the *G* monomer units incorporated into the lignin network, the difference in the percentages between the two samples is relatively low; this could be a potential effect of the genetic modification made – the greater amount of *G* monomers could be offset by the decrease in its decomposition as they are integrated into the polymer via stronger thermally resistant linkages. Few dimethoxy-substituted phenolic

products (i.e. *S* monomer derived thermal product) are detected for both samples. The yield is almost identical for the *G*-derived lignin phenolics products for the low temperature thermal treatment. However, the mutant sample produced approximately 1.6 times lower *S*-lignin derived thermal products as compared to its yield by the isogenic, wild type sample. The primary compound culpable for the majority of this difference was detected to be Syringol,4-vinyl- as the mutant sample produced approximately 75% less as compared to the wild type sample.

Of all the phenolic species identified in the low temperature thermal treatment, the most abundant thermochemical product for both mutant and wild type sample is Phenol,4-vinyl-, which is a *H* monomer derived thermal product; it occupies approximately 40% and 46% of the phenolic thermal product stream for the COMT2 mutant and COMT2 wild type sample respectively. The *H* monomer production pathway is not impacted by the COMT enzyme (7), and as such, the decrease in the *H* monomer derived thermal product within the mutant sample as compared to the wild type is indicative of the fact that a greater portion of the *H* monomer units may have been incorporated into the lignin synthesis network of the biomass via stronger crosslinks as a result of the mutation.

G-monomer derived

compounds identified:

Vanillin
Homovanillin
Eugenol
Isoeugenol (cis/trans)
Guaiacol, 4-vinyl-
Guaiacol, 4-ethyl-
Guaiacol
Guaiacol, 3-methyl-
Guaiacyl acetone

S-monomer derived

compounds identified:

Syringol
Syringol, 4-propenyl- (cis/trans)
Synringol, 4-vinyl-
Syringol, 4-ethyl-
Syringol, 4-methyl-

Figure 4.9: List of organic phenolic species identified through their originating monomer units as used in this study

Figure 4.10: Distribution of phenolic compounds displayed through their originating monomer unit upon torrefaction of COMT2 mutant switchgrass

Figure 4.11: Distribution of phenolic compounds displayed through their originating monomer unit upon torrefaction of COMT2 isogenic, wildtype switchgrass

Figure 4.12: Distribution of phenolic compounds displayed through their originating monomer unit upon pyrolysis of COMT2 mutant switchgrass
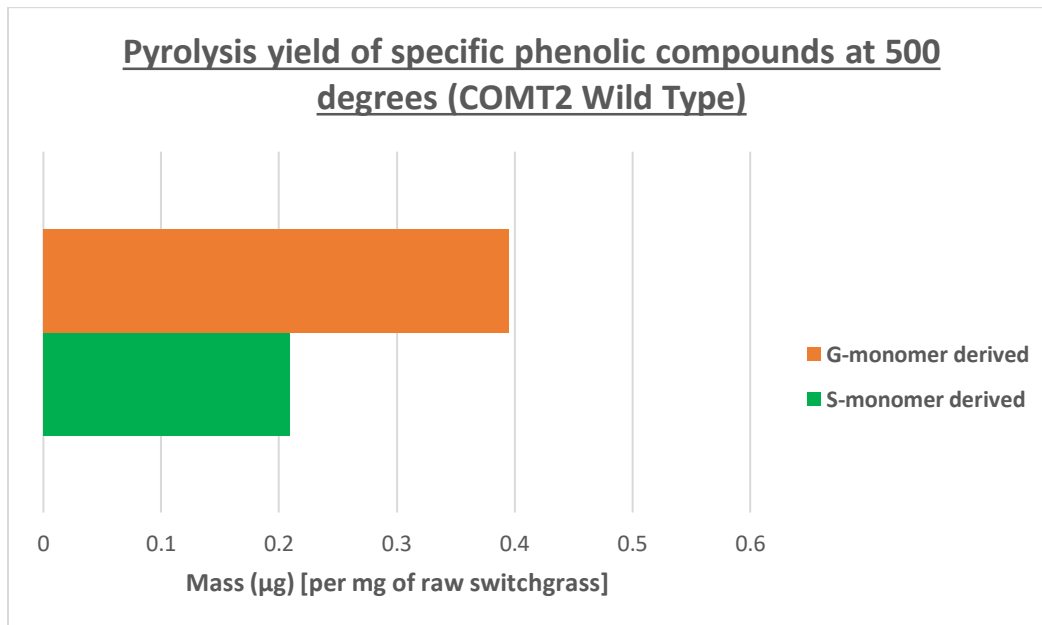
Figure 4.13: Distribution of phenolic compounds displayed through their originating monomer unit upon pyrolysis of COMT2 isogenic, wildtype switchgrass

Figure 4.12 and Figure 4.13 show an expected increase in the quantity of both the *G*-derived and *S*-derived thermal products as a greater portion of the lignin polymeric network is decomposed at higher temperatures. Pyrolysis of the torrefied COMT2 mutant sample results in 0.718 µg (per mg of raw biomass) of *G*-derived and *S*-derived phenolic products as compared to 0.604 µg (per mg of raw biomass) of phenolics from pyrolysis of torrefied COMT2 wild type switchgrass – this represents a 17.25% increase in the phenolic products (only considering the *G*-derived and *S*-derived lignin products) for the mutant switchgrass. This indicates that some lignin decomposition for the mutant sample was suppressed at lower temperatures.

The distribution ratio of the *G*-derived and *S*-derived lignin products (i.e. quantitative and qualitative) observed for both torrefaction and pyrolysis of COMT2 mutant sample were quite similar to the results analyzed from the same degradation treatment of the natural diversity switchgrass sample (both samples contain low *S/G* ratio). The distribution of the lignin products through their originating monomeric units of the natural diversity sample are illustrated in Figure 4.14 and Figure 4.15. The same (i.e. the distribution ratio of *G*-derived and *S*-derived lignin products) cannot be said when results of the isogenic wild type switchgrass and the standard grade AP13 sample (both of which contains high *S/G* ratio) were examined. Upon torrefaction, it was detected that AP13 sample produced double the amount of the *S*-derived lignin phenolics as compared to the wild type sample, while both samples produced approximately an equivalent amount of the *G*-derived phenolics. After pyrolysis, however, it was observed that both samples produced the same amount of *S*-derived phenolics, while the wild type sample produced approximately 1.5 times more of the *G*-derived phenolics. This is illustrated through Figures 4.11, 4.13, and 4.16-4.17.

Figure 4.14: Distribution of phenolic compounds displayed through their originating monomer unit upon torrefaction of natural diversity switchgrass

Figure 4.15: Distribution of phenolic compounds displayed through their originating monomer unit upon pyrolysis of natural diversity switchgrass
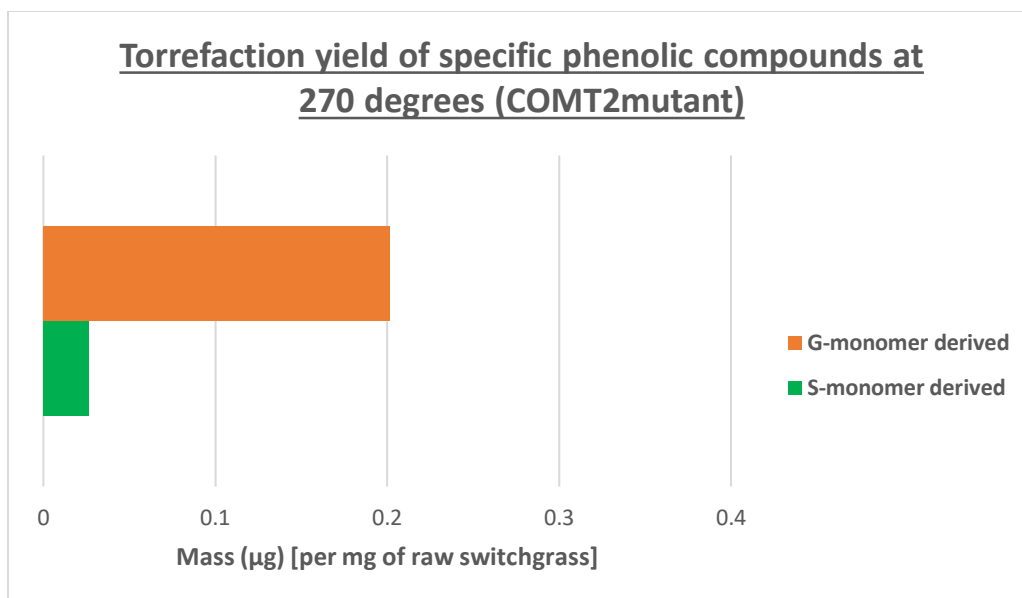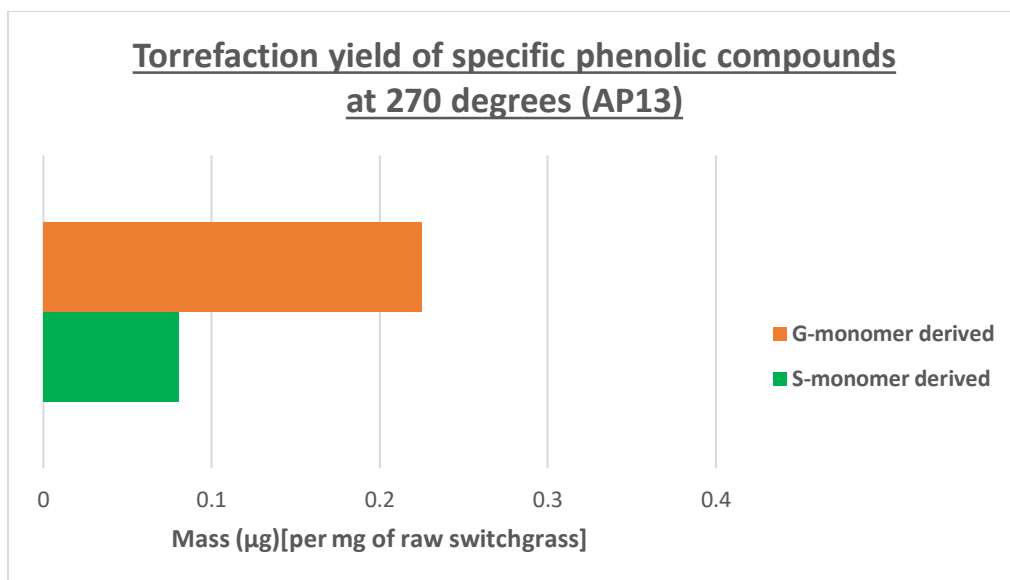
Figure 4.16: Distribution of phenolic compounds displayed through their originating monomer unit upon torrefaction of AP13 switchgrass
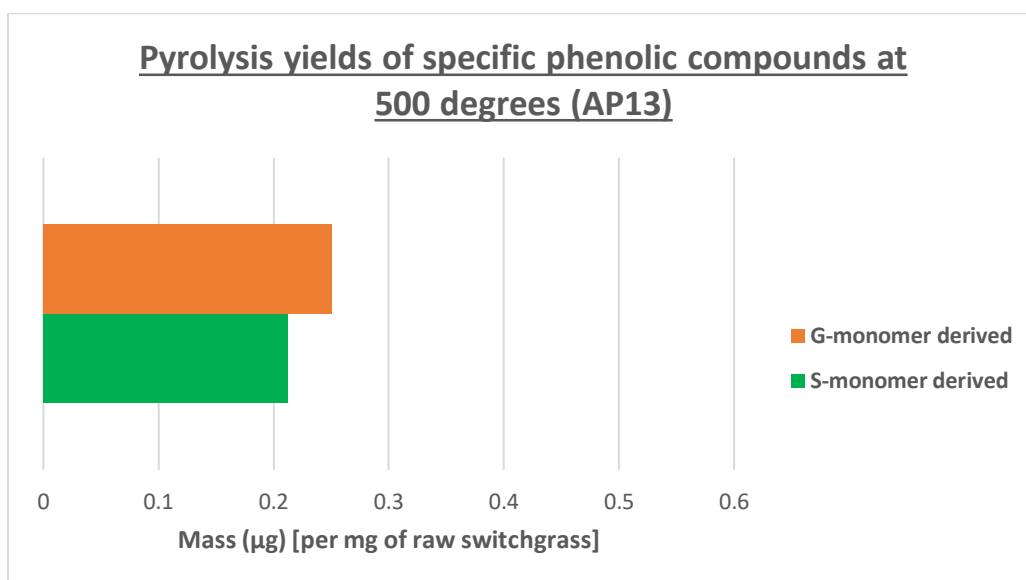
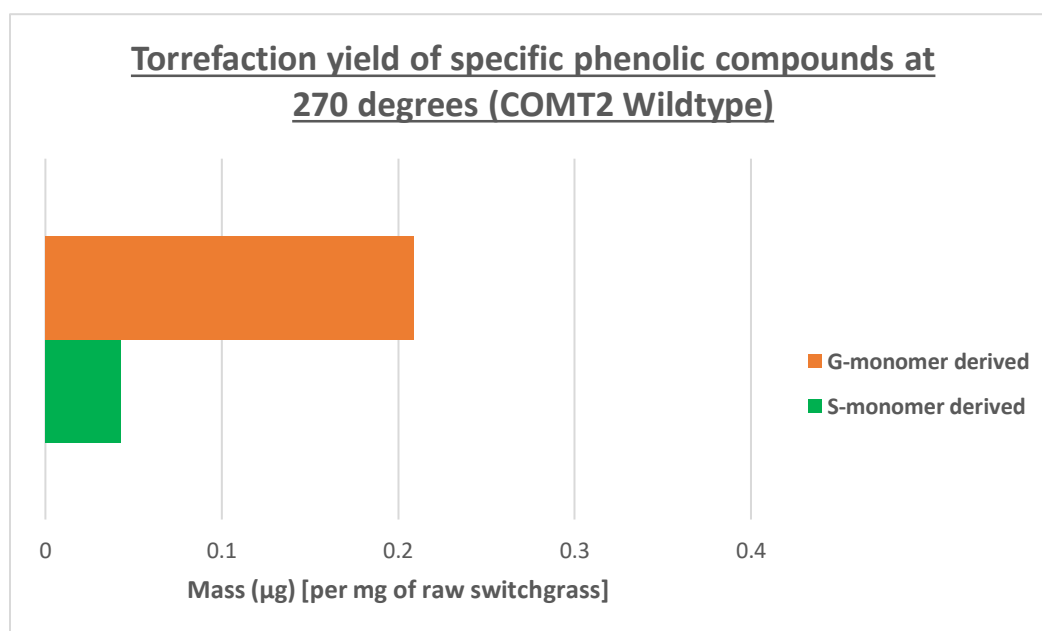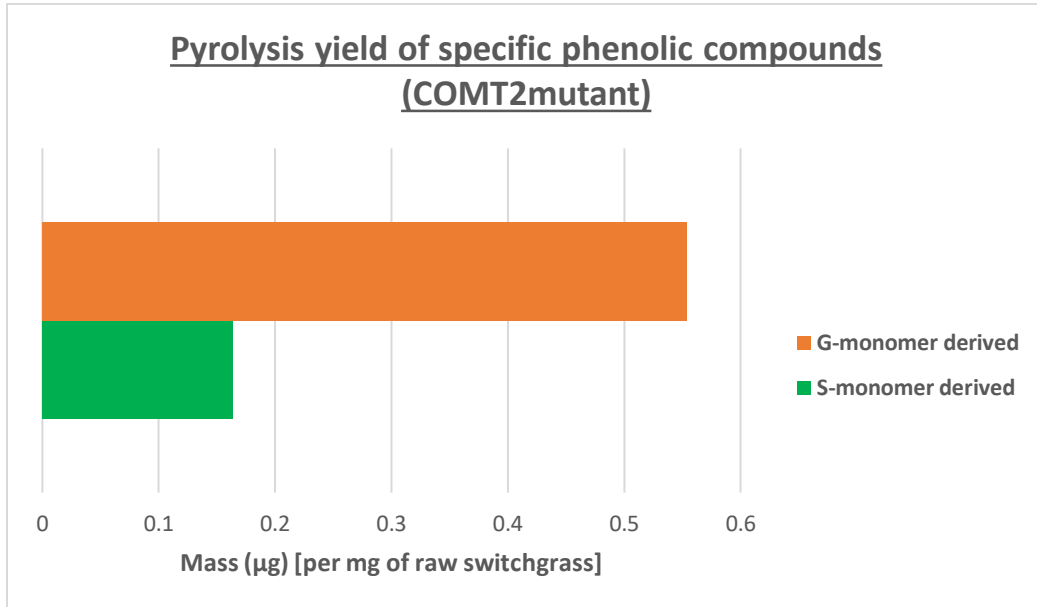**Figure 4.17:** Distribution of phenolic compounds displayed through their originating monomer unit upon pyrolysis of AP13 switchgrass
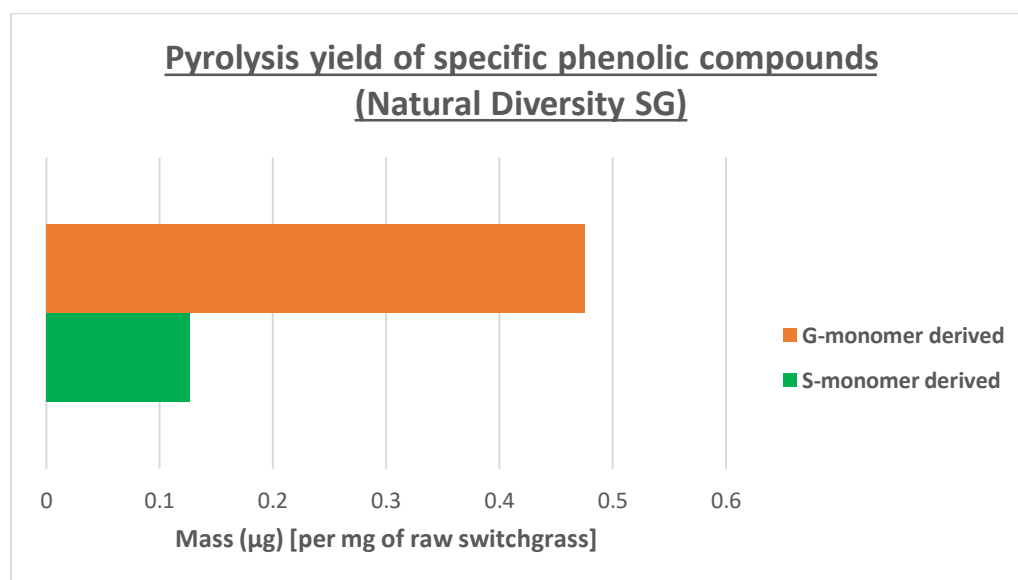
4.5 Discussion
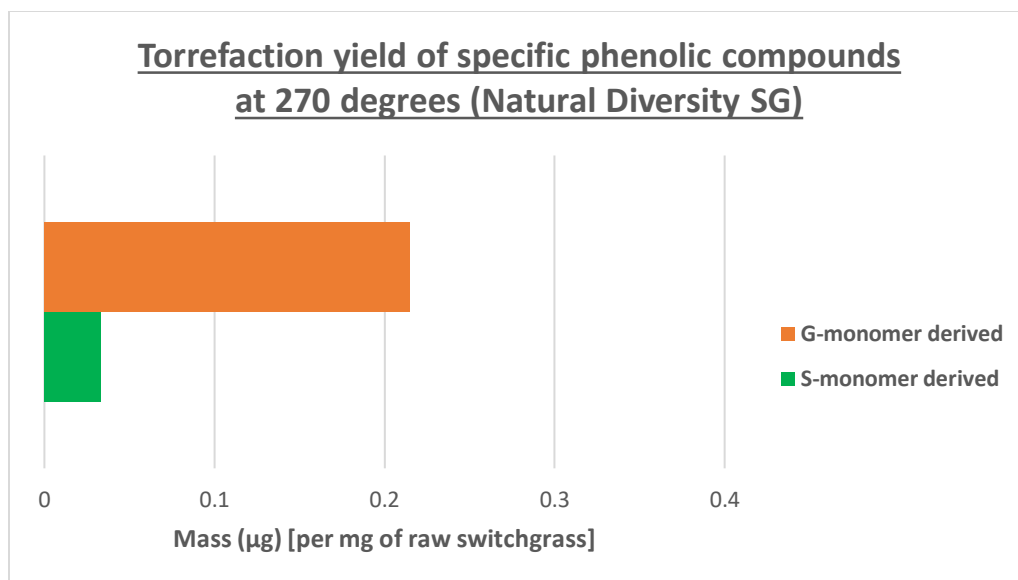
As hypothesized, the COMT2 mutant samples produced less phenolic products than the COMT2 wild type samples when subjected to a low temperature ("Stage 1" as mentioned in chapter 1) thermal degradation treatment for the clean removal of hemicellulose. This observation could be a result of the decreased presence of the β-O-4 (Figure 4.2) inter-unit linkages within the lignin polymeric network due to the suppression of the *S* monomer formation – leading to higher bond dissociation enthalpy distributions- brought about by the genetic modification. The suppression of *S* monomer formation allows the *G* monomer unit to have a greater exposure to the "-5" reaction site; this leads to stronger thermally resistant crosslinks, and thus the low *S/G* ratio samples have a greater fraction of the stronger bonds leading to lesser decomposition at low temperatures. At low temperatures, the most abundant individual thermochemical product in both the wild type and mutant sample is Phenol, 4-vinyl-, which is a *H* monomer derived product. Although the mutant samples were enhanced in *G* monomers, they virtually produced an equivalent amount of the *G* derived phenolics as the wild type samples.

Another plausible explanation for the observed differences in the phenolic yields between the mutant and wild type samples at low temperatures may be due to differing amounts of p-coumaric acid (pCA). It is possible for the genetic modification to lower the levels of pCA within the mutant biomass (an indirect result). Palmer et al. (66) detected low levels of cell wall-bound pCA in a couple variety of COMT-deficient sorghum mutants as opposed to their respective wild types. In conjunction with decreased abundance of pCA, the study also revealed an increase in the levels of ferulic acid (66). The relative decrease in the production of Phenol,4-vinyl- within the mutant switchgrass samples via torrefaction could be attributable to lowered amounts of pCA. However, the COMT2 deficient mutant switchgrass samples produced lower amounts of

Guaiacol,4-vinyl- (discussed above), which is a product of the ferulic acid (7), than the wild type switchgrass. This could be interpreted to assume that the assimilation of the esterified ferulic acid is obtained through the more thermally stable inter-unit linkages. However, this alternative explanation was not examined for the purposes of this thesis since the samples utilized throughout did not have any available data for esterified hydroxycinnamic acids (HCA) measurements. Phenolic products obtained through thermal degradation experiments can come from both HCAs and decomposing polymerized lignin. Hence, it is important to consider the HCA derived phenolic products when any study investigating lignin's thermal stability is examined. Removal of the HCAs from biomass contents can be achieved using a sodium hydroxide extraction technique which allows the lignin polymeric network to be intact. Pretreatment of biomass samples in such a way before subjecting to low temperature thermal degradation would facilitate the comprehension regarding the influence of only heritable traits on observed phenolic thermochemical products as no results would be obscured due to the presence of HCA products.

If the relative abundance of pCA levels are indifferent between the COMT deficient mutant samples and their respective isogenic wild types, then the observed differences in the lowered phenolic products within the mutants via torrefaction is likely due to the magnified thermal stability of the lignin polymeric network incorporated into the cellular framework of the biomass.

References:

1. G. W. Huber, S. Iborra, A. Corma, Synthesis of transportation fuels from biomass: chemistry, catalysts, and engineering. *Chem Rev.* (2006).

2. M. J. C. Stelt, H. Gerhauser, J.H.A. Kiel, K.J. Ptasinski, Biomass upgrading by torrefaction for the production of biofuels: A review. *Biomass and Bioenergy.* (2011).

3. W. Chen, J. Peng, Xiaotao T. Bi, A state-of-the-art review of biomass torrefaction, densification and applications. *Renewable and Sustainable Energy Reviews.* (2015).

4. T. Shahzadi, S. Mehmood, M. Irshad, Z. Anwar, A. Afroz, N. Zeeshan, U. Rashid, K. Sughra, Advances in Lignocellulosic Biotechnology: A Brief Review on Lignocellulosic Biomass and Cellulases. *Advances in Bioscience and Biotechnology.* (2014).

5. P. de Wild, H. Reith, E. Heeres, Biomass pyrolysis for chemicals. *Biofuels.* **2**, 185-208 (2011).

6. Janupala, R. (2016), Staged Thermal Fractionation of Biomass for Segregation of Hemicellulose, Cellulose and Lignin Derived Products (Master of Science), The University of Oklahoma, Norman, USA.

7. Waters, C. (2016), Understanding Thermochemical Process and Feedstock Compositional Impacts on Strategies to Control Pyrolysis and Torrefaction Product Distributions (Doctor of Philosophy), The University of Oklahoma, Norman, USA.

8. W. H. Chen, P. C. Kuo, A study on torrefaction of various biomass materials and its impact on lignocellulosic structure simulated by a thermogravimetry. *Energy.* (2010).

9. H. Yang, R. Yan, H. Chen, D. H. Lee, C. Zheng, Characteristics of hemicellulose, cellulose and lignin pyrolysis. *Fuel.* **86**, 1781-1788 (2007).

10. O. Faix, D. Meier, I. Fortmann, Thermal degradation products of wood: Gas Chromatographic separation and mass spectrometric characterization of monomeric lignin-derived products. Holz als Roh-und Werkstoff (1990).

11. O. Faix, I. Fortmann, J. Bremer, D. Meier, Thermal degradation products of wood: Gas chromatographic separation and mass spectrometric characterization of polysaccharide derived products. Holz als Roh-und Werkstoff (1991).

12. P. J. Dauenhauer, A.D. Paulsen, M.S. Mettler, The Role of Sample Dimension and Temperature in Cellulose Pyrolysis. *Energy & Fuels.* **27**, 2126-2134 (2013).

13. Nhung, D. (2014). Analysis and Catalytic Upgrading of Different Bio-Oil Fractions (Master of Science). The University of Oklahoma, Norman, USA.

14. W. A. Dietz. (1967). Response factors for gass chromatographic analyses. J. *Gas Chromatoge.* **5**, 68-71.

15. Katritzky, A. R.; Ignatchenko, E.S.; Barcock, R. A.; Lobanov, V. S.; Kareison. (1994). Prediction of Gas Chromatographic Retention Times and Response Factors Using a General Quantitative Structure-Property Relationship Treatment. *M. Anal. Chem.* **66**, 1799-1807.

16. Scanlon, J. T.; Willis, D. E. (1985). Calculation of Flame Ionization Detector Relative Response Factors Using the Effective Carbon Number Concept. *J. Chromatogr. Sci.* 23, 333-340.

17. Schofield, K. (2008). The enigmatic mechanism of the flame ionization detector: Its overlooked implications for fossil fuel combustion modeling. *Progress in energy and Combustion Science*. 34, 330-350.

18. Detectors: Flame Ionization Detector – FID. (n.d.) Retrieved from http://www.srigc.com/FID.pdf

19. J.C. Sternberg, W.S. Gallaway, and D.T.L. Jones. (1962). The mechanism of response of flame ionization detectors in Gas Chromatography. N. Brenner, J.E. Callen, and M.D. Weiss, eds. Academic Press, New York, 231-67.

20. Meier, Oassmaa and Peacocke. (1997). Properties of fast pyrolysis liquid: status of test methods. Development in thermochemical biomass conversion, 391-408.

21. P. Tanger, J. L. Field, C. E. Jahn, M. W. DeFoort, J. E. Leach, Biomass for thermochemical conversion: targets and challenges. *Front Plant. Sci.* **4** (2013), doi: 10.3389/fpls.2013.00218.

22. M. A. ONeill, W. S. York, in *Annual Plant Reviews*, J. K. C. Rose, Ed. (John Wiley & Sons, 2009), p. 400.

23. K. P. Vogel *et al.,* Quantifying Actual and Theoretical Ethanol Yields for Switchgrass Strains Using NIRS Analyses. *Bioenerg. Res.* **4**, 96-110 (2011)

24. M. Pauly, K. Keegstra, Cell-wall carbohydrates and their modification as a resource for biofuel. *Plant J.* **54**, 559-568 (2008).

25. C. Somerville, Cellulose Synthesis in Higher Plants. *Annu. Rev. Cell Dev. Biol.* **22**, 53-78 (2006).

26. H. V. Scheller, P. Ulvskov, Hemicelluloses. *Annu Rev Plant Biol.* **61**, 263-289 (2010).

27. M. E. Vega-Sanchez *et al.*, Loss of Cellulose Synthase-Like F6 Function Affects Mixed-Linkage Glucan Deposition, Cell Wall Mechanical Properties, and Defense Responses in

Vegetative Tissues of Rice. *Plant Physiol.* **159**, 56-69 (2012).

28. K. Freudenberg & A.C. Nash (eds) (1968). *Constitution and Biosynthesis of Lignin.* Berlin: Springer-Verlag.

29. W. Boerjan; J. Ralph; M. Baucher (June 2003). "Lignin biosynthesis". *Annu. Rev. Plant Biol.* **54** (1): 519-549. Doi:10. 1146/annurev.arplant.54.031902.134938. PMID 14503002.

30. D. L. Petrik *et al.*, p-Coumaroyl-CoA: monolignol transferase (PMT) acts specifically in the lignin, biosynthetic pathway in Brachypodium distachyon. *Plant J.* **77**, 713-726 (2014).

31. F. Lu *et al.*, Naturally p-Hydroxybenzoylated Lignins in Palms. *Bioenerg. Res.*, 1-19 (2015).

32. R. D. Hatfield, J. M. Marita, K. Frost, Characterization of p-coumarate accumulation, p-coumaroyl transferase, and cell wall changes during the development of corn stems. *J. Sci. Food Agric.* **88**, 2529-2537 (2008).

33. J. Ralph, J. H. Grabber, R. D. Hatfield, Lignin-Ferulate Cross-Links in Grasses- Active Incorporation of Ferulate Polysaccharide Esters into Ryegrass Lignins. *Carbohyd Res.* **275**, 167-178 (1995).

34. W. Lan *et al.*, Tricin, a Flavonoid Monomer in Monocot Lignification. *Plant Physiol.* **167**, 1284-1295 (2015).

35. A. A. Tortosa Masia, B. J. P. Buhre, R. P. Gupta, T. F. Wall, Characterising ash of biomass and waste. *Fuel Processing Technology.* **88**, 1071-1081 (2007).

36. S. V. Vassilev, D. Baxter, L. K. Andersen, C. G. Vassileva, An overview of the chemical composition of biomass. *Fuel.* **89**, 913-933 (2010).

37. O. D. Mante, S. P. Babu, T. E. Amidon, A comprehensive study on relating cell-wall components of lignocellulosic biomass to oxygenated species formed during pyrolysis. *Journal of Analytical and Applied Pyrolysis.* **108**, 56-67 (2014).

38. Mirko Bunzel, john Ralph, Fachuang Lu, A. Ronald D Hatfield, H. Steinhart, Lignins and Ferulate-Coniferyl Alcohol Cross-Coupling Products in Cereal Grains. *J. Agric. Food Chem.* **52**, 6496-6502 (2004).

39. T. -Q. Yuan, S. -N. Sun, F. Xu, R. -C. Sun, Characterization of lignin structures and lignin-carbohydrate complex (LCC) linkages by quantitative 13C abd 2D HSQC NMR spectroscopy. *J. Agric. Food Chem.* **59**, 10604-10614 (2011).

40. F. -X. Collard, J. Blin, A review on pyrolysis of biomass constituents: Mechanisms and composition of the products obtained from the conversion of cellulose, hemicellulose and

lignin. *Renewable and Sustainable Energy Reviews.* **38**, 594-608 (2014).

41. A. Pictet, J. Sarasin, Sur la distillation de la cellulose et de l'amidon sous pression reduite. *Helvetica Chimica Acta* (1918), doi: 10.1002/hlca.19180010109/abstract.

42. A. G. W. Bradbury, Y. Sakai, F. Shafizadeh, A kinetic model for pyrolysis of cellulose. *Journal of Applied Polymer Science.* **23**, 3271-3280 (1979).

43. P. R. Patwardhan, D. L. Dalluge, B. H. Shanks, Distinguishing primary and secondary reactions of cellulose pyrolysis. Bioresource technology (2011), doi: 10.1016/j.biotech.2011.02.018.

44. F. Shafizadeh, G. D. McGinnis, C. W. Philpot, Thermal degradation of xylan and related model compounds. *Carbohyd Res.* **25**, 23-33 (1972).

45. U. Raisanen, I. Pitkanen, H, Halttunen, Formation of the main degradation compounds from arabinose, xylose, mannose and arabinitol during pyrolysis. *Journal of Thermal Analysis and Calorimetry.* **72**, 481-488 (2003).

46. C. Saiz-Jimenez, J. W. De Leeuw, Lignin pyrolysis products: their structures and their significance as biomarkers. *Organic Geochemistry* (1986).

47. B. W. Penning *et al.*, Validation of PyMBMS as a High-thoroughput Screen for Lignin Abundance in Lignocellulosic Biomass of Grasses. *Bioeneg. Res.* **7**, 899-908 (2014).

48. R. Lou, S. Wu, G. Lv, A. Zhang, Factors Related to Minerals and Ingredients Influencing the Distribution of Pyrolysates Derived from Herbaceous Biomass. *Bioresources* (2013).

49. F. Ronsse, X. Bai, W. Prins, R. C. Brown, Secondary reactions of levoglucosan and char in the fast pyrolysis of cellulose. *Environ. Prog. Sustainable Energy.* **31**, 256-260 (2012).

50. R. Fahmi *et al.*, The effect of alkali metals on combustion and pyrolysis of Lolium and Festuca grasses, switchgrass and willow. *Fuel.* **86**, 1560-1569 (2007).

51. P. R. Patwardhan, J. A. Satrio, R. C. Brown, B. H. Shanks, Influence of inorganic salts on the primary pyrolysis products of cellulose. *Bioresource technology.* **101**, 4646-4655 (2010).

52. M. Kleen, G. Gellerstedt, Influence of Inorganic Species on the Formation of Polysaccharide and Lignin Degradation Products in the Analytical Pyrolysis of Pulps. *Journal of Analytical and Applied Pyrolysis.* **35**, 15-41 (1995).

53. I. -Y. Eom et al., Effect of essential inorganic metals on primary thermal degradation of lignocellulosic biomass. *Bioresource technology.* **104**, 687-694 (2012).

54. J. Zhang *et al.*, Cellulose-Hemicellulose and Cellulose-Lignin Interactions during Fast Pyrolysis. *ACS Sustainable Chem. Eng.* **3**, 293-301 (2015).

55. X. Du *et al.*, Analysis of lignin-carbohydrate and lignin-lignin linkages after hydrolase treatment of xylan-lignin, glucomannan-lignin and glucan-lignin complexes from spruce wood. *Planta.* **239**, 1079-1090 (2014).

56. Z. Jin, K. S. Katsumata, T. B. T. Lam, K. Iiyama, Covalent linkages between cellulose and lignin in cell walls of coniferous and nonconiferous woods. *Biopolymers.* **83**, 103-110 (2006).

57. N. D. Bonawitz, C. Chapple, The Genetics of Lignin Biosynthesis: Connecting Genotype to Phenotype. *Annu. Rev. Genet.* **44**, 337-363 (2010).

58. Q. Zhao, R. A. Dixon, Transcriptional networks for lignin biosynthesis: more complex than we thought? *Trends in Plant Science.* **16**, 227-233 (2011).

59. N. Yamaji, J. F. Ma, A Transporter at the Node Responsible for Intervascular Transfer of Silicon in Rice. *Plant Cell.* **21**, 2878-2883 (2009).

60. R. Zhong, Z. H. Ye, Secondary Cell Walls: Biosynthesis, Patterned Deposition and Transcriptional Regulation. *Plant & cell physiology.* **56**, 195-214 (2015).

61. A. Zheng *et al.*, Effect of torrefaction on structure and fast pyrolysis behavior of corncobs. *Bioresource technology.* **128**, 370-377 (2013).

62. P. A. Horne, P. T. Williams, Influence of temperature on the products from the flash pyrolysis of biomass. *Fuel* (1996).

63. W. H. Chen, P. C. Kuo, Isothermal torrefaction kinetics of hemicellulose, cellulose, lignin and xylan using thermogravimetric analysis. *Energy* (2011), doi: 10.1016/j.energy.2011.09.022.

64. M. J. Antal Jr., G. Varhegyi, Cellulose Pyrolysis Kinetics: The Current State of Knowledge. *Ind. Eng. Chem. Res.* **34**, 703-717 (1995).

65. H. l. Baxter *et al.*, Two-year field analysis of reduced recalcitrance transgenic switchgrass. *Plant Biotechnol J.* **12**, 914-924 (2014).

66. N. A. palmer *et al.*, Genetic background impacts soluble and cell wall-bound aromatics in brown midrib mutants of sorghum. *Planta.* **229**, 115-127 (2008).

Appendix: Supplementary Tables

Table A.1: Individual thermochemical compounds categorized in their compound lumps for this study

Name of the compound	Compound group
Acetic acid	Acetic Acid
2-Propenal	Light Oxygenate
Propanal-2-one	Light Oxygenate
Butanal	Light Oxygenate
1-Penten-3-one	Light Oxygenate
2,3-Butanedione	Light Oxygenate
3-Pentanone	Light Oxygenate
2-Butanone	Light Oxygenate
Hydroxyacetaldehyde	Light Oxygenate
2-Butenal (cis or trans)	Light Oxygenate
2-Hydroxypropanal	Light Oxygenate
Hydroxypropanone	Light Oxygenate
2-Propenoic acid methyl ester	Light Oxygenate
1-Hydroxy-2-butanone	Light Oxygenate
3-Hydroxypropanal	Light Oxygenate
2-Hydroxy-3-oxobutanal	Light Oxygenate
1-Acetyloxypropane-2-one	Light Oxygenate
2-Hydroxy-butanedial	Light Oxygenate
Butanedial	Light Oxygenate
2,3-Dihydroxyhex-1-ene-4-one	Light Oxygenate
Furan	Furans
2-Methylfuran	Furans
2-Acetylfuran	Furans
2,3-Dihydro Furan	Furans
(2H)-Furan-3-one	Furans
2-Furaldehyde	Furfurals
2-Furfuryl alcohol	Furfurals
5-Methyl-2-furaldehyde	Furfurals
(5H)-Furan-2-one	Furfurals
Dihydro-methyl-furanone	Furfurals
2-Hydroxy-1-methyl-1-cyclopentene-3-one	Furfurals
Methyl-butyraldehyde derivative	Furfurals
gamma-Lactone derivative	Furfurals

gamma-Butyrolactone	Furfurals
5-Hydroxymethyl-2-furaldehyde	Furfurals
4-Cyclopentene-1,3-dione	Furfurals
2-Furoic acid methyl ester	Furfurals
OH-methyl-dihydropyranone	Furfurals
4-Hydroxy-5,6-dihydro-(2H)-pyran-2-one	Furfurals
3-Hydroxy-2-methyl-pyran-4-one	Furfurals
Methyl-dihydro-(2H)-pyran-2-one	Furfurals
Levoglucosan	Anhydrous Sugars
1,4:3,6-Dianhydro-glucopyranose	Anhydrous Sugars
1,6-Anhydro-beta-D-mannopyranose	Anhydrous Sugars
1,5-Anhydro-beta-D-xylofuranose	Anhydrous Sugars
Anhydrosugar: unknown	Anhydrous Sugars
Toluene	Alkyl Benzenes
Phenol	Alkyl Phenols
Styrene	Alkyl Benzenes
Benzene, ethyl-	Alkyl Benzenes
Benzene, 1,2-dimethyl-	Alkyl Benzenes
Benzaldehyde	Alkyl Benzenes
Anisole	Alkyl Benzenes
Benzylalcohol	Alkyl Benzenes
o-Cresol	Alkyl Phenols
Catechol	Alkyl Phenols
Acetophenone	Alkyl Phenols
Phenol, 4-vinyl-	Alkyl Phenols
Phenol, 2,6-dimethyl-	Alkyl Phenols
Phenol, 2-ethyl-	Alkyl Phenols
Benzaldehyde, 4-hydroxy-	Alkyl Benzenes
Guaiacol	Methoxy Phenols
Catechol, 3-methyl-	Alkyl Phenols
Phenol, 4-allyl-	Alkyl Phenols
Phenol, 4-propenyl-	Alkyl Phenols
furan-2-one	Alkyl Benzenes
Phenol, 2-propyl-	Alkyl Phenols

Guaiacol, 3-methyl-	Methoxy Phenols
Guaiacol, 4-vinyl-	Methoxy Phenols
Guaiacol, 3-ethyl	Methoxy Phenols
Vanillin	Methoxy Phenols
Syringol	Methoxy Phenols
Eugenol	Methoxy Phenols
Isoeugenol	Methoxy Phenols
Guaiacol, 4-propyl-	Methoxy Phenols
Homovanillin	Methoxy Phenols
Acetoguaiacone	Methoxy Phenols
Syringol, 4-methyl-	Methoxy Phenols
Vanillic acid	Methoxy Phenols
Guaiacol, 4-(oxy-allyl)-	Methoxy Phenols
Coniferaldehyde	Methoxy Phenols
Syringol, 4-vinyl-	Methoxy Phenols
Guaiacyl acetone	Methoxy Phenols
Propioguaiacone	Methoxy Phenols
Coniferyl alcohol	Methoxy Phenols
Syringol, 3-ethyl-	Methoxy Phenols
Dihydroconiferyl alcohol	Methoxy Phenols
Syringaldehyde	Methoxy Phenols
Syringol, 4-allyl-	Methoxy Phenols
Propioguaiacone, alpha-oxy-	Methoxy Phenols

Syringol, 4-propenyl-	Methoxy Phenols
Syringol, 4-propyl-	Methoxy Phenols
Homosyringaldehyde	Methoxy Phenols
Acetosyringone	Methoxy Phenols
Syringol, 4-(oxy-allyl)-	Methoxy Phenols
Sinapaldehyde	Methoxy Phenols
Syringyl acetone	Methoxy Phenols
Propiosyringone	Methoxy Phenols
Sinapyl alcohol	Methoxy Phenols
Propiosyringone, alpha-oxy-	Methoxy Phenols

Table A.2: ECN values and their respective Response factors for the identified thermochemical compounds used in this study

Name of compound	ECN value	Response Factor (μg/area)
Furan	3.7662	1.150E-04
2-Propenal	1.9031	1.874E-04
Propanal-2-one	1.9031	2.410E-04
2-Methylfuran	4.6105	1.133E-04
Butanal	2.8876	1.588E-04
Unknown: similar to 1-Penten-3-one	3.8720	1.382E-04
2,3-Butanedione	1.8373	2.981E-04
Unknown: similar to 3-Pentanone	3.8720	1.415E-04
2-Butanone	2.8876	1.588E-04
Hydroxyacetaldehyde	0.4117	9.283E-04
2-Butenal (cis or trans)	2.8876	1.544E-04
2-Hydroxypropanal	1.3166	3.580E-04
Acetic acid	0.6845	5.584E-04
Hydroxypropanone	1.3962	3.376E-04
2-Oxo-propanoic acid methyl ester	1.446	4.497E-04
3-Methylfuran	4.6105	1.133E-04
2-Propenoic acid methyl ester	2.4949	2.196E-04
1-Hydroxy-2-butanone	2.3806	3.355E-04
3-Hydroxypropanal	1.3962	3.376E-04
(3H)-Furan-2-one	1.3829	3.869E-04
(2H)-Furan-3-one	1.3829	3.869E-04
Butanedial	1.8373	2.981E-04
2-Hydroxy-3-oxobutanal	1.2508	5.194E-04
2-Furaldehyde	2.3674	2.583E-04
2-Furfuryl alcohol	2.9107	2.145E-04
1-Acetyloxypropane-2-one	2.4291	3.042E-04
Tetrahydro-4-methyl-3-furanone	4.2699	1.492E-04
2-Acetylfuran	4.6849	1.496E-04
Methoxy-dihydrofuran	3.4793	1.831E-04
4-Cyclopentene-1,3-dione	2.8218	2.257E-04
Dihydro-methyl-furanone	2.3674	2.637E-04
Dihydro-methyl-furanone	2.3674	2.637E-04
5-Methyl-2-furaldehyde	3.3518	2.090E-04
Isomer of compound no. 57: unknown	3.2855	2.210E-04
2,3-Dihydroxyhex-1-ene-4-one	3.6834	2.248E-04
Gamma-Butyrolactone	0.9902	5.532E-04
(5H)-Furan-2-one	1.3829	3.869E-04
4-Hydroxy-5,6-dihydro-(2H)-pyran-2-one	3.2855	2.210E-04

Methyl-dihydro-(2H)-pyran-2-one	3.3518	2.128E-04
2-Hydroxy-1-methyl-1-cyclopentene-3-one	4.2699	1.671E-04
OH-methyl-dihydropyranone	4.2699	1.909E-04
2-Furoic acid methyl ester	2.9591	2.712E-04
3-Hydroxy-2-methyl-pyran-4-one	2.7653	2.902E-04
Methyl-butyraldehyde derivative	3.8720	1.415E-04
Similar to 3-Methyl-(5H)-furan-2-one	2.3674	2.637E-04
Gamma-Lactone derivative	0.9902	5.532E-04
Anhydrosugar: unknown	1.1378	9.069E-04
4-hydroxy-3-methyl-(5H)-furanone	1.3171	5.513E-04
1,4:3,6-Dianhydro-glucopyranose	0.8062	1.138E-03
1,5-Anhydro-arabinofuranose	0.7399	1.136E-03
5-Hydroxymethyl-2-furaldehyde (HMF)	2.8449	2.821E-04
2-Hydroxy-butanedial	1.2508	5.194E-04
2-Hydroxymethyl-5-hydroxy-2,3-dihydro-(4H)-pyran-4-one	0.7537	1.217E-03
1,5-Anhydro-beta-D-xylofuranose	0.7399	1.136E-03
1,6-Anhydro-beta-D-mannopyranose	1.1378	9.069E-04
Levoglucosan	1.1378	9.069E-04
1,6-Anhydro-alpha-d-galactofuranose	-0.3669	-2.813E-03
2,3-Dihydro Furan	3.8520	1.158E-04
1,6-Heptadien-4-ol (NIST11)	0	N/A
Carbon Dioxide	0	N/A
Levoglucosenone	0.3425	2.343E-03
Propanol	1.9031	2.008E-04
4-Methyl-2-hexanone	5.8409	1.243E-04
Formic acid	0.1775	1.651E-03
Propanoic acid	1.6689	2.824E-04
Furfuryl alcohol	2.8437	2.195E-04
3-Methyl-2,5-furandione	2.7360	2.607E-04
2-Methylpropene	2.9534	9.490E-05
4H-Pyran-4-one	3.7004	1.652E-04
Methyl furan-3-carboxylate	4.2922	1.870E-04
5-Hydroxymethyl furfural	2.9457	2.725E-04
2-Butenoic acid methyl ester	3.4793	1.831E-04
3-Methylbutanal	3.8720	1.415E-04
2,4-Dimethylfuran	5.4547	1.121E-04
2,5-Dimethylfuran	5.4547	1.121E-04
2-Methylpropanal	2.8876	1.566E-04
1,2,3-Trimethylbenzene	8.6027	8.885E-05
Acetone	1.9031	1.941E-04
2-Methyltetrahydrofuran	4.6105	1.188E-04
Benzene	5.6493	8.795E-05
Phenol	4.8243	1.241E-04

Toluene	6.6338	8.834E-05
Styrene	7.4780	8.859E-05
Benzene, ethyl-	7.4780	9.029E-05
Benzene, 1,3-/1,4-dimethyl-	7.3378	9.201E-05
Benzene, 1,2-dimethyl-	7.3378	9.201E-05
Benzaldehyde	5.5836	1.209E-04
Anisole	5.6302	1.222E-04
Benzylalcohol	6.1268	1.123E-04
o-Cresol	5.6685	1.214E-04
m-/p-Cresol	5.6685	1.214E-04
Catechol	3.9992	1.752E-04
Acetophenone	6.5680	1.164E-04
Phenol, 4-vinyl-	6.6530	1.149E-04
Anisole, 3-/4-methyl-	6.4745	1.200E-04
Phenol, 2,6-dimethyl-	6.5128	1.193E-04
Phenol, 2-ethyl-	6.6530	1.168E-04
Phenol, 2,4-/2,5-dimethyl-	6.5128	1.193E-04
Phenol, 2,3-dimethyl-	6.5128	1.193E-04
Phenol, 3-ethyl-	6.6530	1.168E-04
Phenol, 3,5-dimethyl-	6.5128	1.193E-04
Phenol, 4-ethyl-	6.6530	1.168E-04
Benzaldehyde, 4-hydroxy-	4.7585	1.633E-04
Guaiacol	4.8052	1.644E-04
Catechol, 3-methyl-	4.8434	1.631E-04
Catechol, 4-methyl-	4.8434	1.631E-04
Phenol, 4-allyl-	7.6374	1.118E-04
Phenol, 4-propenyl- (cis)	7.6374	1.118E-04
Phenol, 4-propenyl- (trans)	7.6374	1.118E-04
Anisole, 2,4-/2,5-dimethyl-	7.3187	1.184E-04
Phenol, 2-propyl-	7.6374	1.134E-04
Phenol, 4-propyl-	7.6374	1.134E-04
Guaiacol, 3-methyl-	5.6494	1.556E-04
Guaiacol, 4-methyl-	5.6494	1.556E-04
Benzoic acid, 4-hydroxy-	4.5243	1.943E-04
Catechol, 3-methoxy-	3.9801	2.241E-04
Guaiacol, 4-vinyl-	6.6339	1.440E-04
Guaiacol, 3-ethyl-	6.6339	1.459E-04
Guaiacol, 4-ethyl-	6.6339	1.459E-04
Vanillin	4.7394	2.043E-04
Syringol	4.7860	2.050E-04
Eugenol	7.6183	1.371E-04
Isoeugenol (cis)	7.6183	1.371E-04
Isoeugenol (trans)	7.6183	1.371E-04
Isoeugenol (different compound)	7.6183	1.371E-04
Guaiacol, 4-propyl-	7.6183	1.388E-04

Homovanillin	5.5836	1.894E-04
Acetoguaiacone	5.7238	1.847E-04
Syringol, 4-methyl-	5.6303	1.901E-04
Vanillic acid	4.5052	2.375E-04
Guaiacol, 4-(oxy-allyl)-	6.7083	1.690E-04
Coniferaldehyde	6.5681	1.726E-04
Syringol, 4-vinyl-	6.6147	1.733E-04
Guaiacyl acetone	6.5681	1.746E-04
Propioguaiacone	6.7083	1.709E-04
Coniferyl alcohol	7.1113	1.612E-04
Coniferyl alcohol (cis)	7.1113	1.612E-04
Coniferyl alcohol (trans)	7.1113	1.612E-04
Syringol, 3-ethyl-	6.6147	1.753E-04
Syringol, 4-ethyl-	6.6147	1.753E-04
Dihydroconiferyl alcohol	7.1113	1.630E-04
Syringaldehyde	4.7203	2.456E-04
Syringol, 4-allyl-	7.5992	1.626E-04
Propioguaiacone, alpha-oxy-	5.6580	2.184E-04
Syringol, 4-propenyl- (cis)	7.5992	1.626E-04
Syringol, 4-propenyl- (trans)	7.5992	1.626E-04
Syringol, 4-propyl-	7.5992	1.643E-04
Homosyringaldehyde	5.7047	2.188E-04
Acetosyringone	5.7047	2.188E-04
Syringol, 4-(oxy-allyl)-	6.6892	2.000E-04
Sinapaldehyde	5.5645	2.381E-04
Syringyl acetone	6.5489	2.043E-04
Propiosyringone	6.6892	2.000E-04
Sinapyl alcohol	7.0922	1.886E-04
Sinapyl alcohol (cis)	7.0922	1.886E-04
Sinapyl alcohol (trans)	7.0922	1.886E-04
Dihydrosinapyl alcohol	7.0922	1.904E-04
Propiosyringone, alpha-oxy-	5.6389	2.530E-04